GENETICS, 2025, 230(4), iyaf106
https://doi.org/10.1093/genetics/iyaf106
Advance Access Publication Date: 3 June 2025
Investigation

# A unified framework governing the establishment and maintenance of transgenerational epigenetic inheritance

Rachel M. Woodhouse,[1,2,†] Natalya Frolows,[1,†] Dhruv S. Monteiro,[1] Jessica J. Hawes,[1] Azelle Hawdon,[1,3,4] Michael Davies,[1] Owen Watson,[1] Victoria S. Lennox,[1] Alyson Ashe[1,*]

[1]Charles Perkins Centre, School of Life and Environmental Science, The University of Sydney, Sydney, NSW 2050, Australia
[2]Division of Genome Science and Cancer, the John Curtin School of Medical Research, The Australian National University, Canberra, ACT 2601, Australia
[3]Embryology, Monash IVF, Melbourne 3121, Australia
[4]Australian Regenerative Medicine Institute, Monash University, Clayton, Victoria 3168, Australia

*Corresponding author: Charles Perkins Centre, School of Life and Environmental Science, The University of Sydney, Sydney, NSW 2050, Australia.
Email: alyson.ashe@sydney.edu.au
[†]Joint first authors.

Transgenerational epigenetic inheritance (TEI) is the transfer of nongenetic information between generations. In *Caenorhabditis elegans*, RNA interference (RNAi) is a conserved process initiated by double-stranded RNA, which can induce TEI. While many factors have been implicated in TEI, whether they act in establishment or maintenance of the transgenerational signal, and the generation in which they act, has not been defined. Here, we characterize the actions of *glh-1*, *hrde-1*, *−2*, *−4*, *morc-1*, *nrde-1*, *−2*, *−4*, *set-25*, *−32*, *wago-1*, *−4*, *znfx-1*, *pup-1*, and *emb-4* within RNAi-induced TEI. We show that these genes can be classified into 3 groups: those involved in only establishment or maintenance, or those involved in both. We identify a heterochromatin-based pathway established in the P0 generation by histone methyltransferases and maintained in later generations by MORC-1, upstream of HRDE-1-dependent silencing. By investigating lineage dynamics, we provide evidence that inheritance patterns are partially determined in RNAi-exposed parents, but that variation between offspring also contributes. And finally, we demonstrate that polyUG RNAs broadly correlate with, but do not define, inheritance patterns. Together, this work forms a cohesive model of RNAi-induced TEI.

**Keywords:** epigenetics; *C. elegans*; chromatin; small RNA; epigenetic inheritance; WormBase

## Introduction

Epigenetic mechanisms are factors other than the sequence of DNA that act to modulate gene expression. These mechanisms are tightly regulated and in many organisms reprogrammed significantly during gametogenesis and early development (Feng *et al.* 2010). However, examples of inherited changes in phenotype or gene regulation in a manner independent of genetic changes have been observed, suggesting that epigenetic mechanisms are not always entirely erased between generations (Feng *et al.* 2010; Skvortsova *et al.* 2018). In *Caenorhabditis elegans*, such gene silencing can be inherited for multiple generations (Ashe *et al.* 2012; Rechavi *et al.* 2014), but the molecular mechanisms underpinning this inheritance are not well characterized.

Several genes have been implicated in transgenerational epigenetic inheritance (TEI), however these genes have been discovered by multiple laboratories across several different paradigms including variations of RNA interference (RNAi)-induced TEI (Vastenhouw *et al.* 2006; Ashe *et al.* 2012; Buckley *et al.* 2012; Akay *et al.* 2017; Spracklin *et al.* 2017; Newman *et al.* 2018; Wan *et al.* 2018), piRNA-induced TEI (RNAe) (Luteijn *et al.* 2012; Shirayama *et al.* 2012), TEI of lifespan extension (Greer *et al.* 2011, 2016; Lee *et al.* 2019), mortal germline (Greer *et al.* 2014; Kerr *et al.* 2014; Lev *et al.* 2017; Spracklin *et al.* 2017), and more (Rechavi *et al.* 2014; Schott *et al.* 2014; Klosin *et al.* 2017; Minkina and Hunter 2017; Camacho *et al.* 2018; Moore *et al.* 2019; Kaletsky *et al.* 2020; Pereira *et al.* 2020; Wan *et al.* 2021). While a handful of factors have been implicated across paradigms, it is unclear whether these different paradigms rely on a common molecular pathway, or whether different pathways contribute to different inheritance paradigms.

RNAi is initiated through the introduction of dsRNA that is processed by Dicer into primary sRNAs. These primary sRNAs complex with argonaute proteins such as RDE-1 and target complementary mRNAs. Subsequently, the endonuclease RDE-8 mediates mRNA cleavage and the recruitment of RDE-3 (Tsai *et al.* 2015), which produces poly-UG RNAs by 3′ UG tailing (Shukla *et al.* 2020); and RNA-dependent RNA polymerases (Tsai *et al.* 2015), which produce 22 nucleotide long secondary siRNAs with a 5′ G bias (22Gs) (Gu *et al.* 2009). The secondary siRNAs associate with additional argonaute proteins, trigger the degradation of complementary transcripts and mediate gene silencing. For some loci, this silencing is maintained for many generations after

Received on 25 February 2025; accepted on 23 May 2025

the removal of the dsRNA. It is hypothesized that a molecular signal must be produced within the RNAi-exposed generation to establish a state of epigenetic silencing that can bypass normal developmental reprograming (establishment), and this may be related to levels of HSF-1 in the parental generation (Houri-Zeevi *et al.* 2020). Furthermore, successive generations must have mechanisms to receive this signal to allow them to maintain and propagate this silenced state (maintenance) (Woodhouse *et al.* 2018). Although histone methyltransferases, other nuclear machinery, cytoplasmic RNA pathway components (including poly-UG RNAs) and germ granules (Ashe *et al.* 2012; Wan *et al.* 2018; Woodhouse *et al.* 2018; Shukla *et al.* 2020; Sundby *et al.* 2021) have all been implicated in this process, it remains poorly understood, particularly the differentiation between establishment and maintenance of silencing. Recently, it has been suggested that 2 pathways—nuclear (requiring *hrde-1*) and cytoplasmic (requiring *znfx-1*)—are both required for efficient TEI and work in parallel (Ouyang *et al.* 2022).

In this study, we investigate a range of proteins and characterize their generational requirements within RNAi-induced TEI to discover their role in establishing or maintaining the transgenerational silencing signal. We identify a heterochromatin-based pathway established in the P0 generation by histone methyltransferases and maintained in later generations by MORC-1, upstream of HRDE-1-dependent silencing. We also examine the long-term dynamics of TEI, showing that animals display heterogeneous inheritance responses, and investigate poly-UG RNAs, demonstrating that these molecules are crucial to the establishment and maintenance of TEI as well as germ granule stability, but do not correlate with silencing longevity. Finally, we form a cohesive model of TEI in *C. elegans*.

# Methods

## Cultivation and maintenance of *C. elegans*

*C. elegans* strains (Supplementary Table 1) were cultured according to standard procedures (Brenner 1974). Unless otherwise specified, animals were grown on Nematode Growth Medium (NGM) (2% (w/v) agar, 50 mM NaCl, 0.25% (w/v) peptone, 1 mM $CaCl_2$, 5 µg/mL cholesterol, 25 mM $K_3PO_4$, and 1 mM $MgSO_4$) seeded with *E. coli* strain OP50. Experiments were performed at 20°C. SX461 was used as the wild-type, which is Bristol strain N2 carrying the TEI sensor *mjIs31[ppie-1::gfp::h2b]*. The sensor is an integrated transgene, which expresses a histone (*h2b*)-GFP fusion protein under the control of the germline-specific promoter *pie-1*.

## RNAi inheritance assays

RNAi was performed by feeding as previously described (Kamath *et al.* 2000). HT115(DE3) bacteria carrying IPTG-inducible L4440-*gfp* or L4440 (empty vector) plasmids was grown with 100 µg/mL ampicillin at 37°C for 7–8 h with shaking. Cultures were seeded on NGM plates containing 25 µg/mL carbenicillin and 1 mM IPTG and grown overnight at room temperature. Day 1 adults were plated onto RNAi bacteria the next day to produce the RNAi-exposed P0 generation. In every experiment, an equal number of replicates were fed on empty vector bacteria as a control, and 0% of empty vector P0 animals were GFP-silenced (data not shown). After 4 days silenced adults were transferred to OP50 plates to produce subsequent generations, unexposed to RNAi. In each generation, 25 day 1 adult animal were randomly selected for scoring from across the plate, representing offspring from the middle of the brood. Animals were scored for the presence of GFP using a Nikon SMZ18 Microscope with Nikon Intensilight C-HGF1 Lamp. Scoring was performed blind to the genotype of the strain by experts in the assay. If a replicate (plate) displayed 0% silencing in a particular generation, no silenced animals could be selected to create the next generation and so the replicate was not continued. Mutants were tested in batches, and so some wild-type control values are shared between figure panels.

To determine the duration of TEI, 8 F1 plates were selected, which showed a range of silencing proportions. Two to five silenced adults from each of the selected F1 plates were plated individually onto OP50 plates to create the F2 generation (termed sublineages). All sublineages were then maintained generation to generation by transferring a single silenced adult to a new OP50 plate every 4 days until silencing inheritance had ceased and the entire population was GFP-expressing. Presence of GFP was scored at every generation.

To test for a requirement in the P0 lineage, 1 silenced mutant hermaphrodite was selected from each P0 plate and placed on a separate NGM plate seeded with OP50 alongside 4–5 unexposed males. These males were wild-type for all loci and had a *gfp* transgene inserted stably into the genome under the control of a pharynx-specific promoter. The plates were incubated at 20°C overnight, allowing the males to cross with the hermaphrodites. The following day the mutant hermaphrodites were moved to new NGM plates with OP50 and incubated at 20°C. As crossing was conducted when the P0 hermaphrodites were young adults, the first few eggs laid were the result of self-fertilization. This means the F1 progeny produced on that day consisted of a mix of self-progeny and cross-progeny. The progeny produced by the crossed P0 hermaphrodites on the second day, after being transferred to a new plate, were comprised entirely of cross-progeny. Cross-progeny were identified based on the presence of pharyngeal GFP and were scored upon reaching adulthood. To generate uncrossed controls, silenced mutant P0 hermaphrodites were transferred to NGM plates seeded with OP50 and their self-progeny scored upon reaching adulthood.

To test for requirement in the F1 generation for *rde-3* or *emb-4*, mutant (*rde-3*(*ne298*) or *emb-4*(*sa44*)) L4 hermaphrodites were crossed to wild-type males on OP50 plates (5 plates per biological replicate, 2 biological replicates). Twenty-four hours later, fertilized adult hermaphrodites were plated onto RNAi bacteria plates prepared as above. Four days later adult hermaphrodites were transferred to OP50 plates to produce the F1 generation (10 plates per biological replicate). After 3 days, P0 adults were scored for silencing then lysed and genotyped to confirm heterozygosity. F1 offspring were scored for silencing and lysed and genotyped (~40 silenced and 40 nonsilenced per biological replicate). Scoring was performed blind to the genotype of the strains.

## CRISPR-Cas9

All projects used CRISPR-Cas9 crRNA and tracrRNA and Cas9 protein as a ribonucleoprotein complex. All projects used a single stranded oligonucleotide repair template. crRNAs, tracrRNAs, and repair templates (Ultramer® DNA Oligos) were ordered from IDT. Cas9 nuclease included a C-terminal SV40-NLS and 6xHis tag, and was expressed from the plasmid pHO4d-Cas9 (Addgene plasmid #67881, a gift from Michael Nonet; Fu *et al.* 2014), and produced by Protein Production and Characterization at Sydney Analytical (University of Sydney).

crRNAs were designed using the IDT Custom Alt-R® CRISPR-Cas9 guide RNA design tool https://sg.idtdna.com/site/order/designtool/index/CRISPR_CUSTOM. crRNAs were selected based on proximity to the edit site, presence of 3′ GG(NGG) (Farboud and Meyer 2015) or G(NGG), and IDT on-target and off-target score.

For *hrde-2*(*smb64*), *hrde-4*(*smb66*), *znfx-1*(*smb69*), and *cec-3*(*smb70*), single stranded oligonucleotide repair templates with 30–50 bp homology arms (Paix *et al.* 2014) were used to generate predicted null mutations. Each repair template incorporated 1 or more premature stop codons, a mutation at the PAM site or several mutations in the guide sequence to prevent cleavage of the repair template, and mutation(s) to introduce a restriction enzyme cleavage site for ease of identifying edited animals. *Hrde-2*(*smb64*) has a stop codon and a PvuII site in the first exon. The *hrde-4*(*smb66*) has a stop codon and a BamHI site in the second exon. *znfx-1*(*smb69*) has a stop codon and an EcoRI site in the first exon of isoform 2a, which is the sixth exon of isoform 2b, and a single base deletion to alter the reading frame in case of stop codon read-through. *cec-3*(*smb70*) has a stop codon and an EcoRI site in the second exon.

For *hrde-2*(*smb64*) and *hrde-4*(*smb66*), we used a *dpy-10* co-CRISPR strategy (Arribere *et al.* 2014). Injection mixes were adapted from the Dernburg lab (Köhler and Dernburg 2016) and included 15.5 µM tracrRNA, 14.3 µM target crRNA, 5 µM *dpy-10* crRNA, 7 µM Cas9 protein, 6 µM target repair (for all except *damt-1*(*smb67*)), and 0.5 µM *dpy-10* repair. To prepare the mix, the tracrRNA and crRNA were incubated at 95°C for 5 min then 20°C for 5 min to hybridize the gRNA complex. Cas9 was incubated with the gRNA at 37°C for 15 min to form the ribonucleoprotein complex. The repair templates were then added at room temperature. Mixes were injected into the gonads of young adult SX461 *mjIs31[ppie-1::gfp::h2b]* animals. Injected animals were grown at 20°C or 25°C and offspring were screened at L4-adulthood for the dpy or rol phenotypes. Dpy/rol animals were genotyped by PCR and restriction enzyme digest to identify successfully edited animals.

For *znfx-1*(*smb69*) and *cec-3*(*smb70*), we used an alternative *zen-4* co-CRISPR strategy (Farboud *et al.* 2019) as these loci are tightly linked to *dpy-10*. Injection mixes included 30 µM tracrRNA, 15 µM target crRNA, 15 µM *zen-4* crRNA, 7 µM Cas9 protein, 6 µM target repair, and 6 µM *zen-4* repair. Mixes were prepared as for *dpy-10* mixes and were injected into the gonads of young adult AKA234 *mjIs31[ppie-1::gfp::h2b]; zen-4*(*cle10*ts) animals. Injected animals were grown at 15°C for 24 h, then transferred to 25°C and grown for a further 3 days as previously described (Farboud *et al.* 2019). Alive (*zen-4*-repaired) animals were genotyped by PCR and restriction enzyme digest to identify successfully edited animals.

For all projects, correct editing was confirmed by Sanger sequencing. Edited strains were outcrossed 1–3 times to remove the dpy mutation where applicable and potential background mutations. crRNA and repair template sequences are included in Supplementary Table 2.

## Poly-UG PCRs

Total RNA was extracted using TRIzol™ Reagent (Invitrogen™, 15596018). After chloroform addition, the upper aqueous phase was purified using the RNA Clean and Concentrator kit (Zymo Research, no. R1013) including the DNAse treatment; 1–5 µg of total RNA (always the same amount for every sample within an assay) and 50 pmol of poly-AC primer with adaptors was used to generate cDNA using the Superscript III First-Strand Synthesis System (Invitrogen, 18080051) including the optional RNAse H step. 1 µl of cDNA was used for the first nested PCR (10 µl volume) performed with MyTaq DNA polymerase (Bioline, BIO-21105). Oligonucleotides used are listed in Supplementary Table 3. First PCRs were diluted 1:100 in MilliQ water and 1 µl of this was used as the template for the second nested PCR. Each PCR underwent 25 cycles of amplification, optimized such that pUG bands were consistently produced in positive control conditions while preserving differences in band intensity between test conditions. *gsa-1*, a *C. elegans* gene with an 18nt long genomically encoded TG repeat, was used as the control for all PCRs (excluding the bacteria only PCRs). PCRs were run on 2% agarose gels at 100 V for 30 min. For Sanger sequencing, bands of interest were cut from agarose gels as marked and extracted using the Zymoclean Gel DNA Recovery Kit. Samples were Sanger sequenced using the GFP secondary PCR forward primer.

## Granule imaging

### *Spinning disk microscopy*

Live day 1 adult animals were mounted onto 1% agarose pads saturated in anesthetic buffer (0.5% (w/v) tetramisole hydrochloride and 0.2% (w/v) tricaine methanesulfonate in M9 buffer [22 mM $KH_2PO_4$, 50 mM $Na_2HPO_4$, 86 mM NaCl, 1 mM $MgSO_4$]). Nuclei were imaged at 3 germline regions: the distal tip, pachytene, and loop using a 3i Marianas Multimodal spinning disc microscope using a 100XC/1.49 Oil TIRF objective. Animals were imaged quickly after mounting to avoid granule degradation. Sequential Z stacks were obtained for each sample. The excitation wavelengths were set to 594 nm at 100 mW laser power for mCardinal, 560 nm at 200 mW for TagRFP and 488 nm at 300 mW for GFP, with 150 ms exposure for each channel.

### *Image analysis*

SVI Huygens professional was used for image deconvolution, with the manual background value set to 100 for all samples. FIJI/ImageJ was used for analysis. A single plane containing cross-sections of nuclei was selected from each Z stack. Individual nuclei were selected ($n = 20$ per pachytene and distal tip, $n = 10$ per loop) and the "Analyze Particles" function was used to quantify the number of detected granules as well as their area and integrated density. Integrated density was corrected to corrected total cell fluorescence (CTCF) using the background mean of each image. Data was plotted using GraphPad Prism v10.1.2. Brown–Forsythe and Welch ANOVA tests were used to determine significance with Dunnett's T3 test used to correct for multiple comparisons.

## Statistical analysis

Statistical analyses as indicated in figure legends were performed using GraphPad Prism. Statistical significance was defined as $P < 0.05$. Error bars indicate standard error of the mean as stated in figure legends.

# Results

## The network of genes required in establishment vs maintenance of TEI

To expand the molecular pathway of RNAi-induced TEI, we identified a variety of genes previously implicated in a range of heritable silencing paradigms (Supplementary Table 4) and tested all factors that did not display an RNAi defective phenotype within our RNAi-induced TEI system (Table 1). In this system, a *pie-1::GFP::his-58* transgene is silenced by RNAi and silencing is subsequently inherited for at least 4 generations after removal of the animals from the RNAi trigger (Fig. 1a). Silencing of GFP provided a visual marker of inheritance: animals in which TEI was maintained inherited silencing and did not express GFP, while animals which failed to inherit the epigenetic signal expressed GFP.

**Table 1.** TEI implicated genes examined in this study.

| Gene | Predicted protein domain/function | Result | Generational requirement |
|---|---|---|---|
| RNAi against a germline-expressed gene | | | |
| *glh-1* | DEAD-box RNA helicase, required for P granule formation (Spracklin *et al.* 2017; Chen *et al.* 2022) | Establishment and maintenance | P0, possible F1 |
| *hrde-2/ enri-3*[a] | Nuclear RNAi factor, controls HRDE-1 RNA loading specificity in the SIMR foci (Spracklin *et al.* 2017; Lewis *et al.* 2020) | Maintenance | F1 only |
| *hrde-4* | Unknown (Spracklin *et al.* 2017) | Establishment and maintenance | P0, possible F1 |
| *morc-1* | Member of GHKL ATPase family. Compacts chromatin (Spracklin *et al.* 2017; Weiser *et al.* 2017) | Establishment and maintenance | P0, possible F1 |
| *nrde-1*[a,b] | Nuclear RNAi factor (Buckley *et al.* 2012) | Likely establishment and maintenance | |
| *nrde-2*[a,b] | Nuclear RNAi factor (Burton *et al.* 2011; Ashe *et al.* 2012; Buckley *et al.* 2012; Luteijn *et al.* 2012) | Establishment and maintenance (also Ashe *et al.* 2012) | P0, possible F1 |
| *nrde-4*[a,b] | Nuclear RNAi factor(Buckley *et al.* 2012) | Likely establishment and maintenance | |
| *pup-1/cid-1/ cde-1* | Poly(U) polymerase, adds uracils to 3′ termini of RNAs (Spracklin *et al.* 2017; Xu *et al.* 2018) | Establishment and maintenance | P0, possible F1 |
| *set-25*[a] | H3K9me3 methyltransferase (Ashe *et al.* 2012; Kalinava *et al.* 2017; Lev *et al.* 2017; McMurchy *et al.* 2017; Woodhouse *et al.* 2018) | Establishment (Woodhouse *et al.* 2018) | P0 only |
| *set-32*[a] | H3K23 methyltransferase (Kalinava *et al.* 2017; Spracklin *et al.* 2017; Kalinava *et al.* 2018; Woodhouse *et al.* 2018; Schwartz-Orbach *et al.* 2020) | Establishment (Woodhouse *et al.* 2018) | P0 only |
| *wago–4*[b] | Germline cytoplasmic Argonaute (binds 22G-RNAs) (Wan *et al.* 2018; Xu *et al.* 2018; Lev *et al.* 2019) | Establishment and maintenance | P0, possible F1 |
| *wago-9/ hrde-1*[a] | Germline nuclear Argonaute (binds 22G-RNAs) (Ashe *et al.* 2012; Bagijn *et al.* 2012; Buckley *et al.* 2012; Luteijn *et al.* 2012; Shirayama *et al.* 2012) | Maintenance (also Ashe *et al.* 2012) | F1 only |
| *znfx-1*[a] | Helicase domain protein, key Z granule component (Ishidate *et al.* 2018; Wan *et al.* 2018; Ouyang *et al.* 2022) | Establishment and maintenance | P0, possible F1 |
| RNAi against a germline-expressed gene in an RNAi-enhanced genetic background | | | |
| *hda-4* | Class II histone deacetylase (Vastenhouw *et al.* 2006) | Not required (Ashe *et al.* 2012) | |
| *isw-1* | Chromatin remodeling factor (Vastenhouw *et al.* 2006) | Not required (reduction of function mutant) | |
| *mrg-1* | Chromodomain-containing protein (Vastenhouw *et al.* 2006) | Not required (Ashe *et al.* 2012) | |
| RNAi against a somatically expressed gene (intergenerational inheritance) | | | |
| *mp-3* | Small nuclear ribonucleic protein-specific splicing factor (Newman *et al.* 2018) | Not required | |
| RNAe | | | |
| *emb-4* | ATPase with an RNA helicase domain (Akay *et al.* 2017) | Establishment | P0 only |
| *hpl-2* | Chromodomain-containing protein, interacts with H3K9 methylation (Ashe *et al.* 2012; Shirayama *et al.* 2012) | Not required | |
| *let-418* | PHD and chromodomain-containing protein, nucleosome remodeling component of the NuRD and Mec complexes (McMurchy *et al.* 2017) | Not required | |
| *lin-61* | MBT-containing protein, interacts with H3K9 methylation(McMurchy *et al.* 2017) | Not required | |
| *mes-3* | Subunit of polycomb repressive complex 2 (PRC2), which deposits H3K27 methylation (Shirayama *et al.* 2012) | Not required in reduction of function mutant | |
| *mut-2/rde-3* | Ribonucleotidyltransferase, adds poly(UG) tails to 3′ termini of RNAs | Initiation, establishment, and maintenance; RNAi defective | P0 and F1 |
| *wago-1* | Germline cytoplasmic Argonaute (binds 22G-RNAs) | Establishment and maintenance | P0, possible F1 |

[a]Also RNAe.
[b]Also RNAi against a somatically expressed gene (intergenerational inheritance).

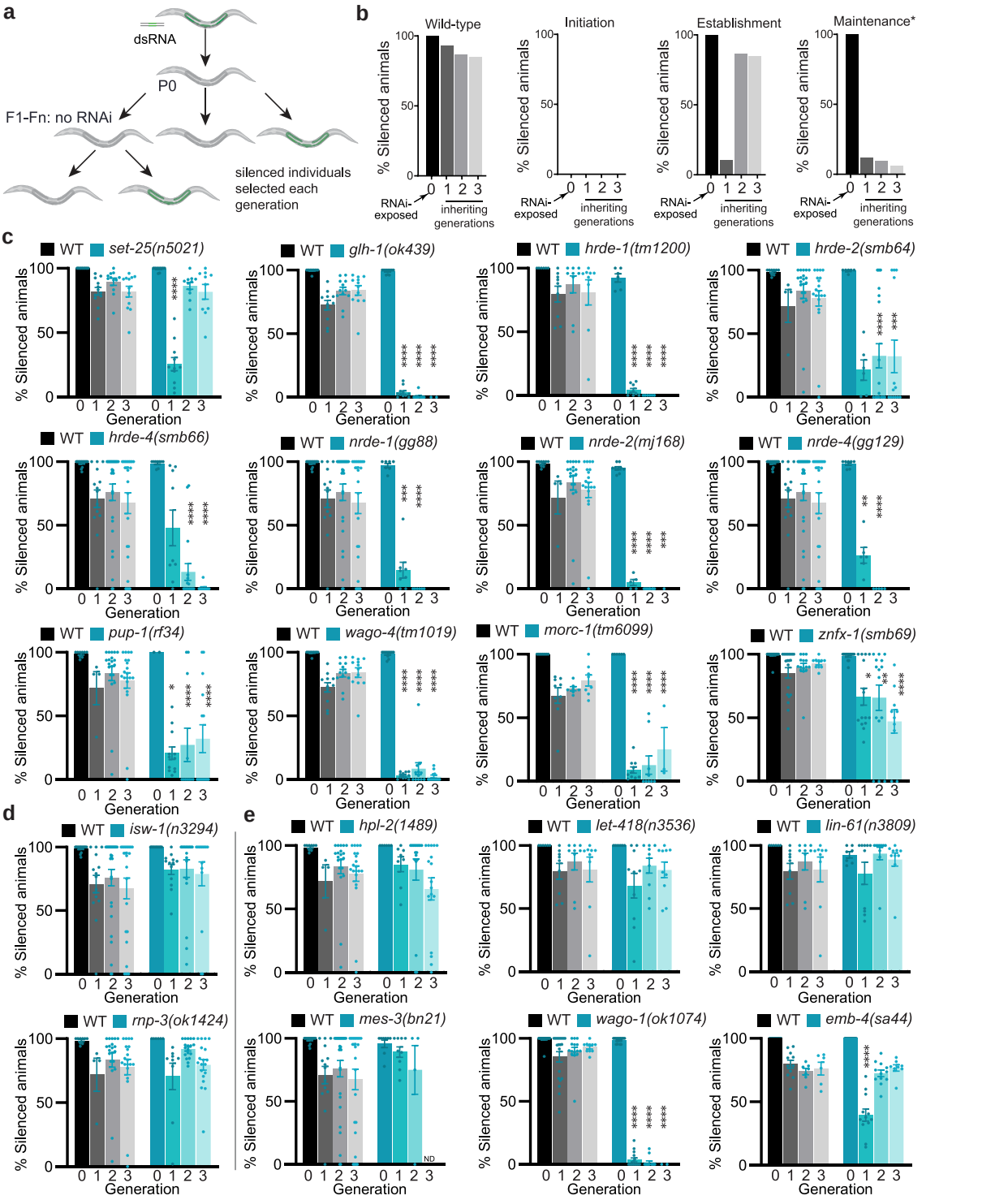


**Fig. 1.** Testing genes in the RNAi-induced TEI sensor system. a) Schematic of system to quantify RNAi-induced TEI. The sensor strain contains a nuclear germline-expressed GFP transgene. GFP-expressing animals are represented in green and GFP-silenced animals are represented in gray. The P0 generation is exposed to RNAi by feeding with bacteria expressing dsRNA complementary to GFP. Subsequent generations are produced by selecting silenced individuals and allowing them to self-reproduce. These generations are not exposed to RNAi. b) Example graphs showing the percentage of GFP-silenced animals in each generation in wild-type animals, and those expected from animals containing mutations in genes required for either initiation, establishment, or maintenance of TEI. Adapted from Woodhouse and Ashe (2019). *May also indicate a role in both establishment and maintenance (c) TEI sensor assays of genes previously implicated in RNAi-induced silencing of germline-expressed genes. SET-25 TEI assay data have been previously published (Woodhouse *et al.* 2018) and so was included as a control. d) TEI sensor assays of genes implicated RNAi inheritance in a sensitized background or against somatically expressed genes. e) TEI sensor assays of genes implicated in RNAe. *mes-3*(*bn21*) displayed increasing sterility with successive generations and so only 4 replicates were scored in F2, and no replicates could be scored in F3 (all selected parents were sterile; ND, not done). c-e) The mean (+/−SEM) percentage of silenced animals is shown for each generation, with dots showing individual biological replicates. $N = 9–15$ plates per strain, 25 animals scored per plate across 3 biological replicates. Mutants were tested in batches, and so some wild-type control values are shared between panels. Comparisons between strains and wild-type were performed by two-way ANOVA with Sidak's post hoc test. Only statistically significant comparisons are displayed. *$P < 0.05$, **$P < 0.01$, ***$P < 0.001$, ****$P < 0.0001$.

We chose to categorize animals in a binary system to ensure that we did not discriminate between levels of expression (Supplementary Fig. 1a). Crucially, we selected completely silenced individuals to create each subsequent generation. This allowed us to probe the genetic requirements in each generation, and distinguish establishment and maintenance factors (Fig. 1a and b). While subtle silencing defects may exist in some strains, our categorical approach allowed us to robustly track the inheritance of epigenetic silencing across multiple generations. We have previously defined establishment factors as those required in the P0 generation only and not required in subsequent generations for TEI, and maintenance factors as those required in the F1 and beyond (Woodhouse *et al.* 2018). In our assay, establishment and maintenance factors show distinct silencing profiles as demonstrated in Fig. 1b.

Genes previously observed to be required for TEI in assays silencing germline-expressed genes (*glh-1*, *hrde-1*, *hrde-2*, *hrde-4*, *nrde-1*, *nrde-2*, *nrde-4*, *pup-1*, *wago-4*, *morc-1*, and *znfx-1*) (Fig. 1c and Table 1) were crucial for functional TEI within our system and displayed a pattern of inheritance indicative of a role in "maintenance" or "establishment and maintenance." Most displayed a very strong phenotype, except for *znfx-1*, which showed a weaker maintenance defect, perhaps indicating that *znfx-1* is part of a parallel or redundant silencing pathway while the other genes are essential (Ouyang *et al.* 2022). The strength of the *znfx-1* defect appears to be allele specific as *znfx-1*(*gg561*), a deletion mutant, shows a more severe phenotype than early stop codon mutants *znfx-1*(*gk58570*) (Wan *et al.* 2018) and our novel *znfx-1*(*smb69*). Genes which had been shown to have a role in inheritance of RNAi in a sensitized background, or a role in RNAi against somatically expressed genes did not display a role in TEI in this assay (Fig. 1d and Table 1; Ashe *et al* 2012). Most of the genes implicated in RNAe (*hpl-2*, *let-418*, *lin-61*, *mes-3*, and *prg-1*) were not required for TEI in this system (Fig. 1d and Table 1; Ashe *et al.* 2012). However, *emb-4* and *wago-1* were both required for TEI in our hands, for establishment and maintenance, respectively. Heterochromatin-associated proteins, *cec-3* and *hpl-1*, were also not required for RNAi-induced TEI (Supplementary Fig. 1). Novel null mutants for *hrde-2*, *hrde-4*, *cec-3*, and *znfx-1* were used in this assay (Supplementary Fig. 2).

While performing these TEI assays, we noticed broad variation in silencing inheritance responses between replicates in some strains. This is surprising, as P0 animals are exposed to an identical RNAi silencing trigger, and offspring are genetically identical. In our control strain, most replicates displayed silencing inheritance of 70–90% in the F1, F2, and F3 generations. However, we observed some replicates with silencing of 100% of assayed individuals, and others displaying very low silencing proportions. Similarly, we observed wide variation in silencing inheritance in some mutant strains, particularly those with medium severity maintenance defects: *pup-1*, *znfx-1*, *hrde-2*, and *hrde-4* (Fig. 1c). Conversely, mutants with severe maintenance defects (*glh-1*, *hrde-1*, *wago-1*, *wago-4*, *nrde-1*, −2, and −4) exhibited little variation, with tight clustering of replicates with very low silencing proportions. Perhaps these severe mutants are essential for TEI, while the less severe mutants contribute to and promote TEI in combination with additional factors and pathways.

## The number of generations that epigenetic memory persists is primarily determined in the P0 parent

To understand the source of this variation, we investigated the long-term dynamics of TEI in wild-type individuals. Studies have previously shown that silencing is able to persist for at least 4 (Ashe *et al.* 2012) or 7 generations (Rechavi *et al.* 2014) depending on the trigger, but neither study continued until silencing was completely exhausted. Reduced GFP expression for over 80 generations has also been observed in an enhanced RNAi genetic background (Vastenhouw *et al.* 2006) but the duration of silencing in a wild-type background has not been well studied. To characterize the dynamics and duration of silencing in the absence of the RNAi trigger, we tracked individual lineages and sublineages by propagating single animals from each population at every generation. We aimed to capture lineages descending from F1 populations displaying the breadth of silencing responses, which we previously observed (0–100%). To this end, we enriched for variation by establishing many independent F1 populations (each from a different P0 parent), and then selecting 8, which encompassed a range of F1 silencing proportions. We named these lineages A-H (Fig. 2a). For each of the 8 lineages, 2 to 5 silenced F1 offspring were transferred to individual plates to create sister "sublineages" derived from the same P0 parent (each sublineage numbered 1–5). We then maintained each of the sublineages by transferring 1 silenced animal at each generation until the entire population expressed GFP. This experimental set up allowed us to simultaneously investigate potential differences in silencing dynamics and duration between independent lineages from different P0 parents, and sister sublineages from the same P0 parent.

We first compared inheritance dynamics in independent lineages from different P0 parents by calculating the mean percentage of silencing inheritance between sister sublineages. Different lineages displayed a wide range of transgenerational inheritance dynamics (Fig. 2b). Three lineages showed relatively weak inheritance, with silencing inherited for between 2 and 5 generations following RNAi (lineage F, G and H). The other 5 lineages showed stronger inheritance, with silencing persisting for between 8 and 10 generations. In this latter group, inheritance proportions were generally high to F5, before displaying a sharp decline in F6 and F7. The proportion of silencing in an F1 population and the maximum duration that silencing persisted in that lineage was strongly correlated (Fig. 2c). The variation in inheritance dynamics between different lineages suggests that independent P0 parents transmit different silencing signals to their descendants, and that a watershed moment occurs around the F6 generation.

We next examined all sublineages (Fig. 2d). In most cases, sublineages descended from a single P0 parent shared similar but not identical inheritance dynamics. For example, all B sublineages showed strong inheritance (>64%) for 5–7 generations, before a dramatic drop in silencing between F6 and F9. One lineage (Fig. 2d, Lineage G) showed identical dynamics: all 3 sublineages failed to inherit silencing beyond F1, each displaying 0% silencing at F2. This similarity between sister sublineages from a single P0 parent again suggests that inheritance dynamics are determined at least in part in each P0 animal, and then transmitted with some degree of consistency to sister F1 sublineages.

However, substantial variation still exists between sister sublineages. We observed examples where sublineage inheritance patterns differed by up to 6 generations (for example Fig. 2d, Lineage D and E). This variation suggests that differences between F1 sisters or their descendants also play a role in determining inheritance dynamics. These differences may be due to inherited variation from P0 parents, or in variation between the F1 sisters or their descendants themselves.

Taken together, these results indicate that RNAi-exposed P0 parents contribute not only to the transmission of gene silencing

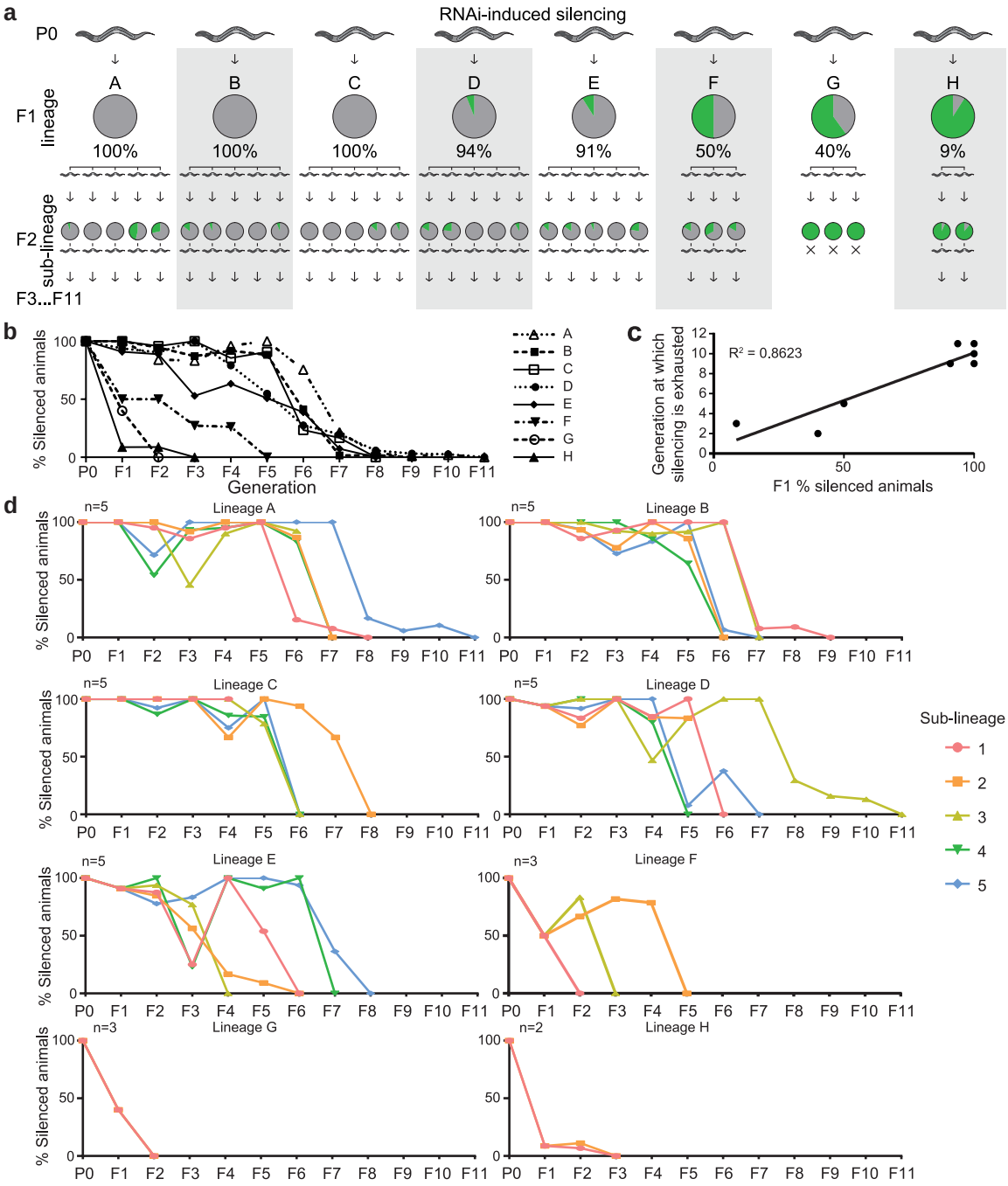


**Fig. 2.** Silencing inheritance dynamics. a) RNAi-exposed GFP-silenced P0 animals were plated individually to produce independent F1 populations, which were not exposed to the RNAi trigger. Eight F1 populations were selected which exhibited a range of silencing proportions. These were termed "lineages" and named (a-h). For each lineage, 2–5 silenced F1 offspring were transferred to individual plates to create sister "sublineages" derived from the same P0 parent. Each sublineage was maintained by transferring a single silenced worm to a new plate every generation until silencing was exhausted. For example, the sublineages from lineage (g) showed 0% silencing at F2, and so were not maintained further. Pie charts at F1 and F2 depict the percentage of animals in each population, which are GFP-silenced (gray) or GFP-expressing (green). b) Mean silencing inheritance dynamics in lineages (a-h). The percentage silencing of sister sublineages within each lineage ($n = 2–5$) were averaged at each generation. c) Relationship between the percentage of silencing in an F1 population and the generation in which all sublineage populations displayed 0% GFP silencing. The relationship appears linear (linear regression constrained to $x = 0$, $y = 1$; $y = 0.092^{*}x + 1$; $R^2 = 0.89$). d) The percentage of GFP-silenced animals produced by the assay in (a). The graphs display results from different lineages derived from different individual P0 parents. Each colored line plots the inheritance in a sublineage. $n = 2–5$ sublineages as marked, 10–27 animals scored per sublineage in each generation.

across generations but also to the inheritance of a factor that influences how long the silencing persists. This factor could represent an additional signal or perhaps the strength of the initial silencing established in the P0 generation.

## polyUG RNAs are necessary but not sufficient for epigenetic inheritance

Poly-UG RNAs (pUGs) are recently identified RNA molecules synthesized by the RNAi defective protein, RDE-3 (Tabara *et al.* 1999;

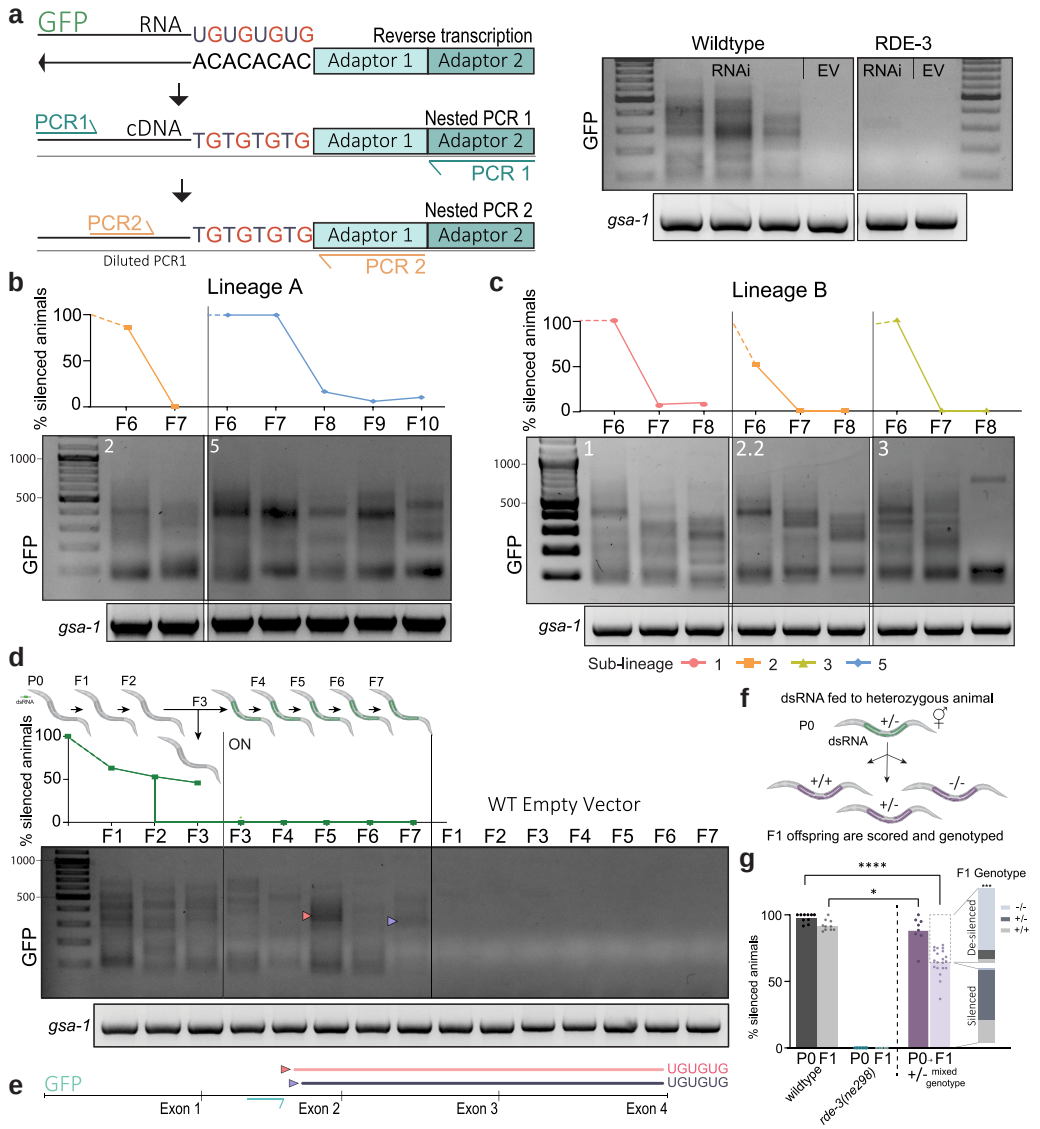


**Fig. 3.** PolyUG RNAs during TEI. a) Schematic of the nested PCR method for amplifying pUGs for agarose gel visualization and an example of expected pUG gel results. b,c) Nested pUG PCRs on indicated sublineages from Fig. 2. Samples were collected from the F6 until the end of silencing. d) Nested pUG PCRs of samples from the modified TEI assay. Animals were selected for silencing of the GFP gene ("OFF") until the F2 generation where progeny were split into ON and OFF lineages. The OFF lineage was collected only until the F3 generation while the ON lineage was collected up to F7. e) Graphical representation of Sanger sequencing of indicated pUG bands from (d). f) Schematic of the F1 heterozygous assay. Animals heterozygous for *rde-3*(*ne298*) were exposed to the RNAi treatment and allowed to produce F1 offspring. These F1 offspring were scored for silencing and genotyped. g) F1 heterozygous TEI assay for *rde-3* mutants. The genotype of the silenced (lilac) and desilenced (dashed line) F1 offspring is represented by bar graphs. $n = 10$ plates per strain, 25 animals were scored on average per plate across 2 biological replicates. A total of 134 offspring of heterozygous animals were scored and genotyped. Comparisons between strains were performed by two-way ANOVA with Tukey's post hoc test.

Shukla *et al.* 2020). RDE-3 activity is required for production of WAGO-class 22G RNAs (Gu *et al.* 2009) and is necessary for the maintenance of RNAe induced silencing (Lee *et al.* 2012). We previously showed that 22G RNAs correlate with RNAi-induced silencing in the P0 generation, but not with silencing in the F1 generation (Woodhouse *et al.* 2018). As RDE-3 reportedly acts in conjunction with RDE-8 to recruit RNA-dependent RNA polymerases (RdRPs) to mRNA (Tsai *et al.* 2015), and pUGs appear to occur upstream of 22G biogenesis, we hypothesized that they may correlate with silencing duration in sublineages and could be the factor in the P0 responsible for lineage variation. In order to assess pUG levels, we modified a previously developed RT-PCR strategy (Shukla *et al.* 2020) (Fig. 3a). We used this strategy to measure pUGs from 2 lineages across the generations during which silencing of the GFP transgene was lost (Fig. 3b and c; Supplementary Fig. 3). If pUGs are the main factor responsible for silencing, their abundance should correlate with the percentage of silencing in a particular generation. For example, consider Lineage B between the F6 and F8 generations: the sublineages that still display high levels of silencing in the F6 generation should have high levels of pUG RNAs, while those in which silencing is already extinct should have low/no pUG RNAs. In contrast, high levels of pUG RNAs were observed in all sublineages (Fig. 3b and c). pUGs also appeared to be present even after silencing had ceased (e.g. Figs. 3b–lineage A and 4c–lineage B), although in some cases they appeared smaller over the generations (e.g. Fig. 3c). The retention of pUGs after loss of silencing was unexpected, as a recent report showed an absence of pUG RNAs after loss of silencing in *prg-1* mutants, and inferred that

the presence of pUGs correlated with silencing (Shukla *et al.* 2021). Given this disparity, we designed an experiment to investigate the dynamics of pUG disappearance after loss of silencing. This modified TEI assay selected for "ON" worms in the F2 generation and followed this "ON" lineage until F7, with all generations collected postscoring (Fig. 3d). In each generation GFP-expressing animals appeared as bright as control EV treated animals. Surprisingly, abundant polyUG RNAs were present for at least 5 generations after silencing was lost and did not disappear during the experiment (Fig. 3d; Supplementary Fig. 3). Indicated bands were excised and subjected to Sanger sequencing, confirming that the bands corresponded to the GFP transgene and contained UG tails (Fig. 3e).

The pUGylase protein RDE-3 is RNAi defective, and therefore pUGs must be acting within the P0 generation when the dsRNA is present. Despite this, pUGs have previously been associated with maintenance of the transgenerational signal (Shukla *et al.* 2020). As pUGs do not appear to correlate with silencing longevity in our hands, we were interested to investigate whether RDE-3 was only required for initiation of the signal in the P0 generation or also for maintenance in the F1. To test this, we designed a F1 generational requirement TEI assay (Fig. 3f) where animals heterozygous for *rde-3* were exposed to the RNAi and allowed to produce F1 offspring, which were scored for silencing and genotyped. If RDE-3 is not required in the F1, we would expect an equal mix of genotypes between the silenced and desilenced F1 s. If RDE-3 is required in the F1 we would expect all homozygous mutant offspring to be desilenced. Homozygous mutant offspring were desilenced in the F1 generation (Fig. 3g) indicating that RDE-3 is required in the F1 to maintain RNAi-induced silencing. This indicates that pUG production is required to maintain silencing, or possibly that *rde-3* is also playing another, as yet uncharacterized, role in heritable silencing.

Taken together, these data demonstrate that although the administration of pUG RNAs is sufficient to initiate silencing (Shukla *et al.* 2020), the continued presence of pUGs in later unexposed generations is not alone sufficient to maintain this silencing. This may be due to a dosage effect, where a threshold level of pUGs is required, due to a sequestration of pUGs into germ granules compartments in later generations or some other molecular factor(s) also being required for efficient silencing. It is possible that the continued presence of pUGs is associated with very weak silencing, not detected in our assay. However, the presence of pUGs even 5 generations after cessation of silencing suggests that additional factors beyond pUGs are required for robust silencing in maintenance generations.

## Determining the generational requirements of epigenetic inheritance factors

Given that polyUG RNAs did not correlate well with silencing duration and are therefore likely not the main factor influencing silencing establishment and maintenance, we aimed to identify other factors acting in the P0 generation, which may define silencing establishment and duration. To this end, we designed a P0 requirement assay to determine the generation in which TEI mutants (identified in Fig. 1) are required. This assay involves the transmission of silencing through a single parental line and so we first confirmed that silencing could be transmitted though both the female (oocyte) and male (sperm) germlines from the P0 to the F1 generation (Supplementary Fig. 4) (as also recently observed by Schreier *et al.* 2024). To perform the assay, homozygous mutant hermaphrodites that had been exposed to anti-GFP RNAi were crossed with unexposed wild-type males, and the phenotype of their heterozygous F1 offspring was compared with wild-type and homozygous mutant F1 populations (Fig. 4a). If heterozygous offspring from a homozygous parent show the same phenotype as homozygous offspring from a homozygous parent, this indicates that the parent's genotype determines the offspring's phenotype, suggesting the gene acts in the P0 generation, or is a maternal effect gene acting early in development before zygotic gene activation. Conversely, if the heterozygous offspring resemble wild-type, this shows that the genotype of the offspring is more important, indicating that the gene's role is not in the P0 generation but in the F1 generation onwards. To differentiate self- from cross-progeny in this assay, we monitored transmission of pharynx-expressed GFP from RNAi-unexposed fathers mated with RNAi-exposed hermaphrodites to detect cross-progeny. It has been previously shown that the pharynx is refractory to RNAi silencing in the P0 generation (Kumsta and Hansen 2012; Ashe *et al.* 2015) but susceptible to silencing in F1 self-progeny from RNAi-exposed hermaphrodites (Shiu and Hunter 2017). In this experiment, we did not observe any silencing of the pharyngeal GFP in F1 cross progeny, confirming that this system was appropriate for our experimental purposes.

Our previous work using an F1 generational requirement assay showed that *set-25* and *set-32* were not required in the F1 generation, indicating activity in the P0 (Woodhouse *et al.* 2018). This same assay also showed that *emb-4* was not required in the F1 generation (Supplementary Fig. 5). Because of this, we included *emb-4*, *set-25* and *set-32* in the P0 requirement assay as controls and the results showed these were required in the P0 generation, as expected (Fig. 4b). We observed that heterozygous F1 individuals from *wago-4*, *glh-1*, *znfx-1*, and *hrde-4* all displayed the same phenotype as the homozygous F1 offspring (Fig. 4c), indicating that the introduction of a wild-type allele at the F1 generation does not rescue the TEI defect and that these genes likely function in the P0 generation. Considering the data from the standard TEI assay in Fig. 1 where these 4 genes showed a maintenance defect and the results from these assays together, these genes likely act in both generations. The heterozygous F1 for *morc-1*, *pup-1*, *wago-1*, and *nrde-2* showed a phenotype in between their wild-type and homozygous mutant counterparts (Fig. 4d), suggesting that these genes have roles in both the P0 and F1 generations. Finally, the heterozygous F1 for *hrde-1* and *hrde-2* were the same as their wild-type counterparts and not the homozygous F1 (Fig. 4e), suggesting that it is sufficient to have a working copy of both in the F1 generation to inherit silencing. Taken together with the data from Fig. 1, which allows us to judge whether genes are required over multiple generations, these data clearly show 3 categories of genes: establishment factors involved in the P0 only (3 genes; mostly chromatin factors), factors required for establishment and maintenance, involved in both the P0 and F1 generations (8 genes; many cytoplasmic RNA pathway components), and maintenance-only factors, not required in P0 (2 genes; nuclear RNAi components).

## Role for establishment factors in polyUG synthesis

Given that pUGs are necessary for TEI and initially synthesized in the P0 generation, we assayed the subset of mutants that are required in the P0 generation for TEI to determine whether they are involved in polyUG biogenesis. We assayed polyUGs in the F1 generation following RNAi treatment in *set-25*, *set-32*, *morc-1*, *hrde-4*, *nrde-2*, *hrde-1*, *emb-4*, *znfx-1*, and *wago-1* mutants. Of these, *znfx-1* has previously been implicated in polyUG biogenesis and shown to result in depleted polyUG levels in F1 individuals

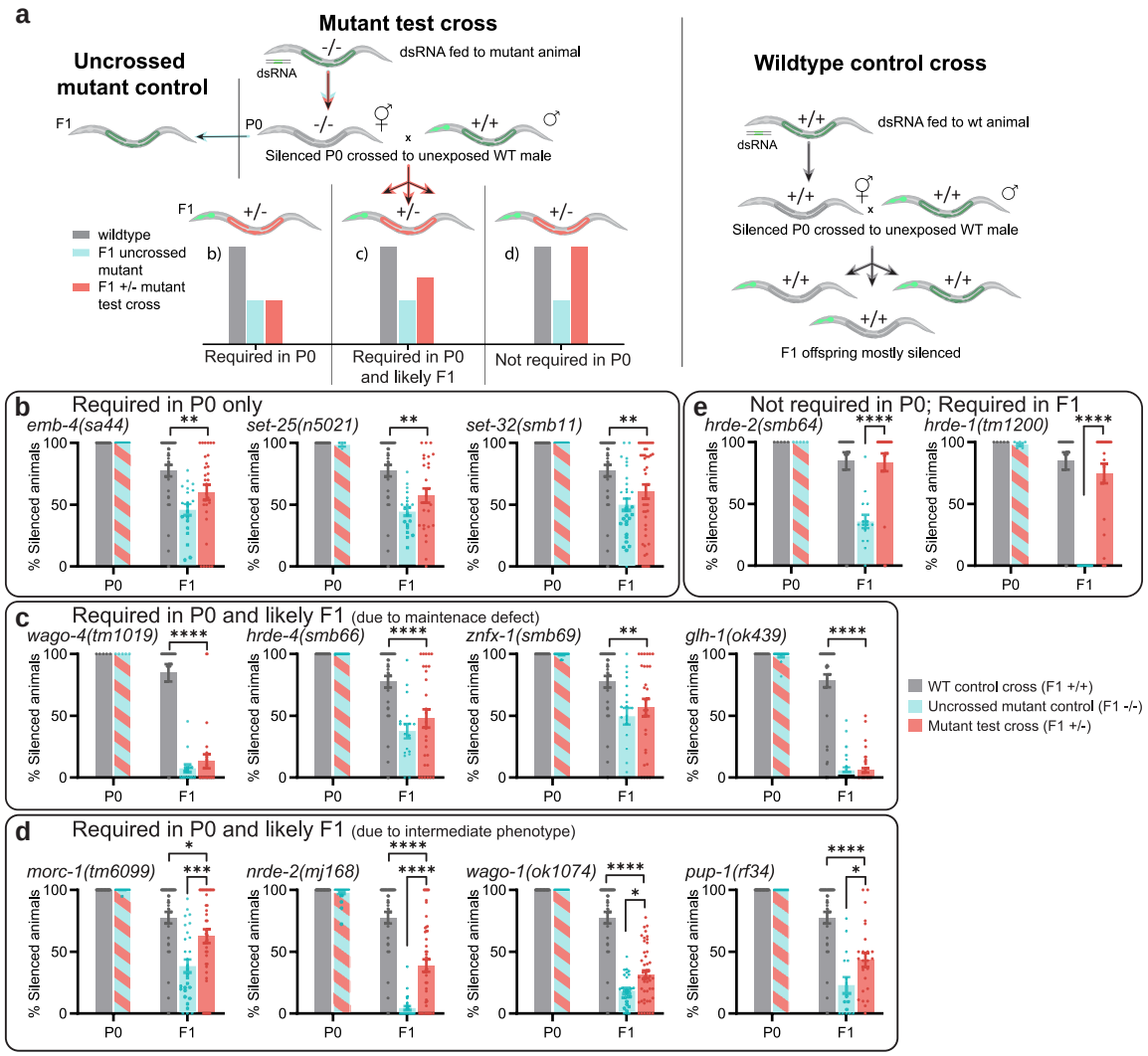


**Fig. 4.** TEI assays with heterozygous F1. a) Schematic showing the control and test crosses to determine the generation in which the genes mediating TEI are required. Mutant hermaphrodites exposed to RNAi for the germline *gfp* transgene are crossed with unexposed wild-type males containing the pharynx *gfp* transgene. The F1 are scored for *gfp* expression, with cross-progeny identified by the presence of pharyngeal *gfp* expression. The wild-type strain crossed to the pharyngeal *gfp* strain and the uncrossed mutant strains were used as controls. b-e) The results for different mutants assessed by the assay in (a). Groupings are based on the results from both the standard TEI assay in Fig. 1c and this assay as follows. b) TEI factors that were confirmed to act only in the P0 generation. These genes are not required for inheritance in the F1 generation (Supplementary Fig. 5 and Woodhouse *et al.* 2018). c) TEI factors that are required in the P0 generation and likely in the F1 generation, as they display maintenance defect in Fig. 1c. d) TEI factors that are required in the P0 generation and probably in the F1 generation, due to their intermediate phenotype in this assay. e) TEI factors that are not required in the P0 generation; the percentage of silenced animals in the F1 mutant test cross were significantly different to the mutant test cross, but not significantly different to the wild-type F1. b-e) The mean (+/−SEM) percentage of silenced animals is shown for each generation, with dots showing individual biological replicates. $N = 10–50$ biological replicates per strain. Mutants were tested in batches, and so some wild-type control values are shared between panels. Comparisons between all strains were performed by two-way ANOVA with Tukey's post hoc test, and only those that are statistically significant with the mutant test cross are displayed. $^{*}P \leq 0.05$, $^{**}P \leq 0.01$, $^{***}P \leq 0.001$, $^{****}P \leq 0.0001$.

(Ouyang *et al.* 2022). We detected polyUG RNAs in all strains, despite all these strains showing a defect in silencing in the F1 generation (Fig. 5a-e). However, the polyUG RNAs appear somewhat depleted in *znfx-1*, *wago-1* and potentially *morc-1* animals (Fig. 5b), somewhat supporting the reported role for *znfx-1* in their biogenesis and suggesting that *wago-1* and *morc-1* may have similar functions. Intriguingly, *hrde-4* mutants appear to have more abundant polyUG RNAs (Fig. 5d), although this observation requires further testing with a quantitative assay.

Overall, we conclude that only some establishment factors play a role in pUG abundance in the F1 generation. This suggests that pUGs sit upstream in the pathway, and/or that they work in conjunction with other pathways.

## RDE-3 affects germ granule morphology

Germ granules are liquid–liquid condensates, which form a complex network on the nuclear periphery and are thought to be major hubs of silencing small RNA amplification and processing (Wan *et al.* 2018; Dodson and Kennedy 2020; Sundby *et al.* 2021; Phillips and Updike 2022; Chen *et al.* 2024). Given that RDE-3 is thought to localize to mutator foci (Phillips *et al.* 2012) and ZNFX-1 is important for both pUG production and Z granule formation (Ouyang *et al.* 2022), we investigated whether RDE-3 is required for germ granule formation and stability within different stages of the *C. elegans* germline.

We assessed germ granules using a strain containing PGL-1::mCardinal (P granules), ZNFX-1::tagRFP (Z granules), and

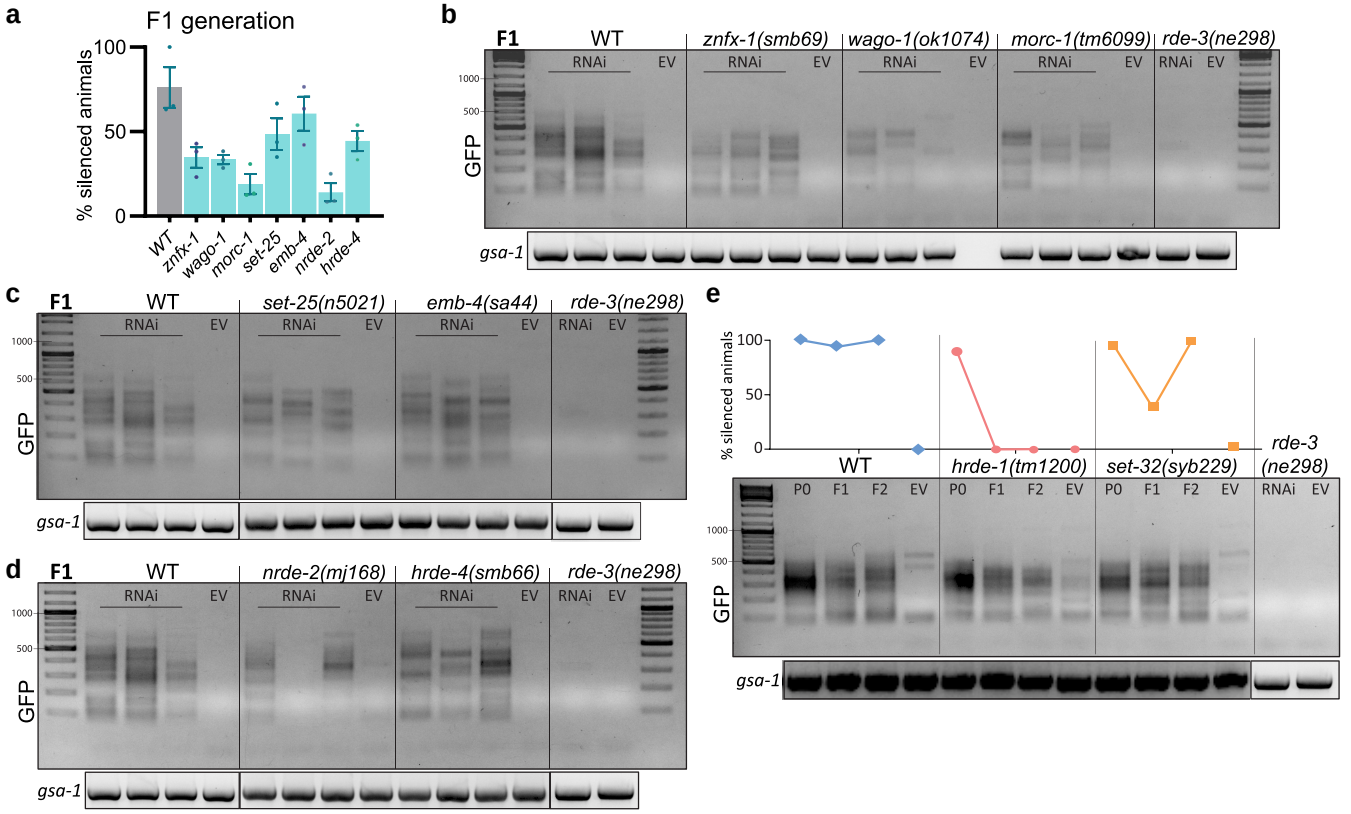


**Fig. 5.** polyUG RNAs in TEI mutants. a) Silencing percentage in the F1 generation for each mutant strain. Dots indicate each replicate shown in (b-d). b-d) Nested pUG PCRs on F1 mutant samples derived from TEI assays from Fig. 1. The WT and *rde-3*, *gsa-1* controls shown are the same samples for each gel. The cDNA reaction failed for the *wago-1* EV sample as evidenced by the *gsa-1* control, so no conclusions can be made about this sample. e) P0-F2 mutant samples for *hrde-1* and *set-32* mutants.

MUT-16::GFP (mutator foci). When compared to wild-type, *rde-3* mutants had significantly less P granules per nucleus in the distal tip and pachytene regions of the germline (Fig. 6a and b). P granules were also significantly smaller and had lower CTCF in the pachytene and loop germline regions, indicating a lower concentration of PGL-1 (Fig. 6c and d). The *rde-3* mutants also had far fewer mutator foci per nucleus in all germline regions with lower CTCF in the pachytene and loop regions and slighter smaller mutator foci in the germline loop region (Fig. 6a and h-J). Interestingly, the number of Z granules in *rde-3* mutants was equivalent to wild-type in the distal tip and pachytene regions and higher than wild-type in the loop region (Fig. 6e), although the granules were smaller and with lower CTCF in the pachytene and loop regions (Fig. 6f and g). Overall, *rde-3* mutants have defects in P granule and mutator foci formation and changes in Z granule morphology.

Mutations in WAGO-1 do not appear to significantly impact the formation of germ granules within the pachytene and distal tip regions of the germline. However, WAGO-1 may play some role in granule morphology as P and Z granules were smaller in mutant animals in some germline regions (Supplementary Fig. 6).

## Discussion

Using our sensitive system for studying TEI, we have characterized its robustness, the role of polyUG RNA and germ granules in this process, and defined a genetic framework and mechanism that incorporates generational requirements. Our findings, together with previous studies, indicate that TEI is governed by a complex system of molecular interactions involving chromatin modifiers, germ granules, and RNA molecules acting across generations to establish and maintain the epigenetic signal. Here, we discuss our findings in the context of a unified framework that explains epigenetic inheritance pathways.

Our results have defined a network of genes that are required for RNAi-induced TEI. As expected, all genes that we tested that had been previously implicated in RNAi-induced TEI against a germline-expressed gene in wild-type background validated in our system. In contrast, we found that only some genes required for RNAe are also required for RNAi-induced TEI. To establish a transgenerational signal in the P0 generation, SET-25 and SET-32 are required to add the heterochromatic histone modifications H3K9me3 and H3K23me3 respectively to the locus to establish a heterochromatic state and compact chromatin (Towbin *et al.* 2012; Schwartz-Orbach *et al.* 2020). These proteins are then dispensable for maintenance of this signal from the F1 generation onwards (Figs. 1, 4, and 7a; Woodhouse *et al.* 2018) suggesting that once the heterochromatic state is established it remains stable over multiple generations. Our findings show that the ATPase MORC-1 is required to maintain and likely also establish the transgenerational signal in both the P0 and F1 generations. MORC-1 forms discrete nuclear foci surrounding regions of heterochromatin (Kim *et al.* 2019) and is required for maintaining localization of heterochromatin to the inner nuclear periphery (Weiser *et al.* 2017). We hypothesize that MORC-1 forms inner nuclear foci that hold heterochromatin close to nuclear pores allowing siRNAs/rare mRNAs from silenced genes to be routed into perinuclear germ granules to maintain long-term silencing.

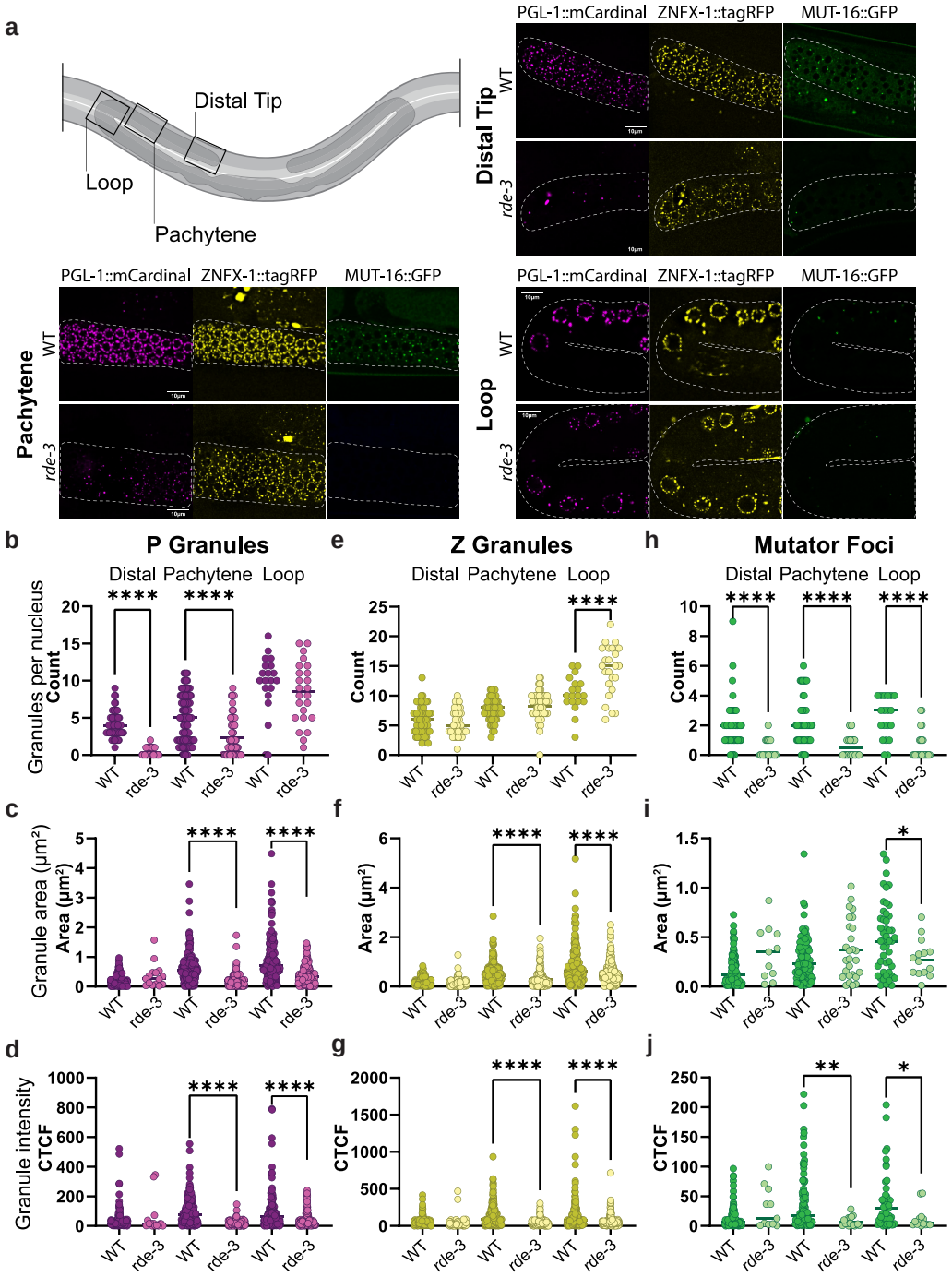


**Fig. 6.** Germ granule perturbations in *rde-3* mutants. a) Schematic of the distal tip, pachytene, and loop germline regions imaged with representative images of the fluorescent tagged proteins surrounding the germline nuclei in the distal tip, pachytene, and loop regions. b–j) Quantification of germ granules in wild-type and RDE-3 mutant germlines. Average number, area, and CTCF of P granules (b–d), Z granules (e–g), and mutator foci (h–j) surrounding individual nuclei in the distal tip, pachytene, and loop regions of the germline. Bar displays the mean. Distal tip and pachytene regions $n = 20$, loop region $n = 10$, per animal for 3 biological replicates. Comparisons were performed using Brown–Forsythe and Welch ANOVA with Dunnett's T3 multiple comparisons test, ****$P \leq 0.0001$. Nonsignificant comparisons are not displayed.

MORC-1, perhaps acting in concert with other chromatin-associated proteins, may help to maintain the heterochromatic state established by SET-25 and SET-32 in the P0 (Fig. 7b).

EMB-4 is required solely in the P0 generation (Fig. 4; Supplementary Fig. 5) and has been suggested to bridge intron gaps allowing small RNA pathways to compete for access to nascent transcripts (Akay *et al.* 2017). EMB-4 physically interacts with HRDE-1 (Akay *et al.* 2017) and its presence represses HRDE-1 small RNA binding, re-routing small RNAs to CSR-1 (Tyc *et al.* 2017). Since we found that the HRDE-1 dependent nuclear RNAi pathway was not required for silencing within the P0 generation but was required in the F1 generation (Fig. 4), the role of EMB-4 within the P0 generation may be to dampen the HRDE-1 pathway, instead allowing nascent transcripts to be shuttled into an establishment pathway (Fig. 7a). This may explain the lack of requirement for EMB-4 in the F1 generation where HRDE-1 plays an important role.

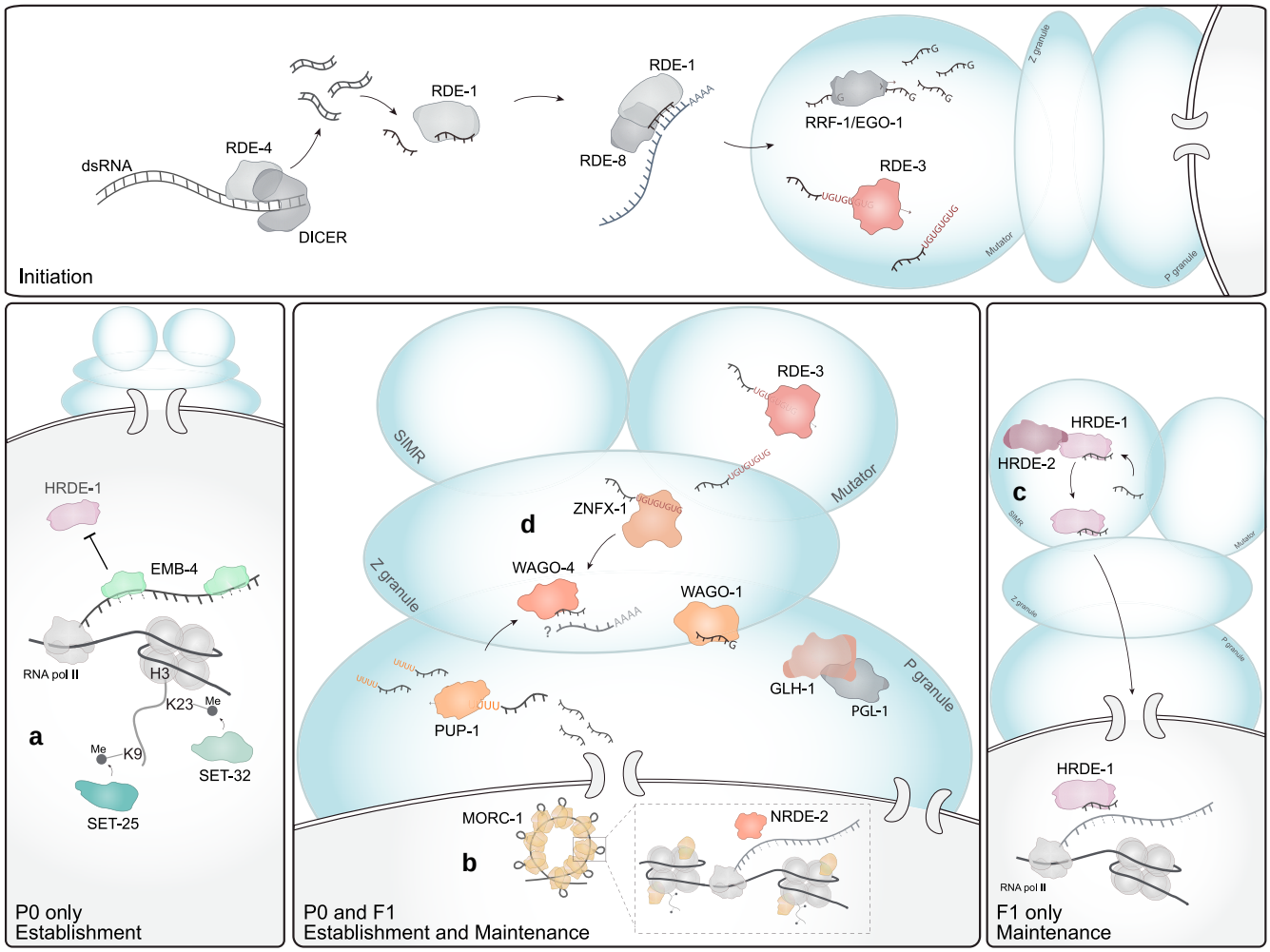


**Fig. 7.** A unified working model of epigenetic inheritance. a) Establishment of a transgenerational epigenetic signal involves chromatin-related proteins in the nucleus in the P0 generation. b) Chromatin compaction and other nuclear factors are required during establishment and maintenance in the P0 and F1 generations. c) HRDE-1 and HRDE-2 play a role in maintenance in the F1 generation only. d) Perinuclear granules are crucial sites for establishment and maintenance in the P0 and F1 generations.

Our results show that HRDE-1 and HRDE-2 act within the F1 generation for maintenance of TEI. HRDE-2 localizes to SIMR foci, a perinuclear germ granule that neighbors Z granules, and is required for the correct loading of 22G RNAs onto HRDE-1 (Chen *et al.* 2024). Unloaded HRDE-1 localizes to SIMR foci and in the absence of HRDE-2, HRDE-1 loads CSR-1 class 22Gs instead of WAGO-class 22Gs (Chen *et al.* 2024). This suggests that HRDE-2 acts to shuttle RNAs to the HRDE-1-dependent TEI maintenance pathway (Fig. 7c), which acts at the cotranscriptional level in the nucleus (Buckley *et al.* 2012). Interestingly, we found that NRDE-2 was required in the P0 as well as the F1 generation even though it has previously been reported to act downstream of HRDE-1 (Ding *et al.* 2023); clearly this protein can act independently of HRDE-1 indicating that the nuclear RNAi machinery is not completely HRDE-1 dependent.

Our finding that HRDE-1 is required only in the F1 generation and thus cannot be solely responsible for the recruitment of NRDE-2 in the P0 generation is curious and contradicts other working models of TEI (Buckley *et al.* 2012; Wan *et al.* 2020; Seroussi *et al.* 2022; Ding *et al.* 2023). However, this has been observed before. Buckley *et al.* showed a similar result using a *pos-1* based RNAi TEI assay, in which the heterozygous offspring of animals that lacked HRDE-1 in the dsRNA exposed generation were able to inherit RNAi silencing (Buckley *et al.* 2012). Furthermore, Schreier *et al.* also observe a role for HRDE-1 in the F1 generation only (Schreier *et al.* 2024). Together, these data suggest that there must be another mechanism governing the recruitment of nuclear RNAi machinery within the P0 generation.

## polyUG RNAs are necessary but not sufficient for epigenetic inheritance

RDE-3, GLH-1, WAGO-1, WAGO-4, ZNFX-1, and PUP-1 all act in both the P0 and F1 generations and reside within perinuclear germ granules (Fig. 7d). RDE-3, the enzyme responsible for adding polyUG tails to RNA molecules, is required for the initiation, establishment, and maintenance of TEI and acts within both the P0 and F1 generations (Fig. 3f). We observed a decrease in the number of mutator foci and P granules in *rde-3* mutant animals, as well as a change in Z granule morphology across many stages of the adult germline, indicating that RDE-3, or the pUGs that it produces, plays a key role in the formation and/or stability of multiple germ granules (Fig. 6). Despite all this, pUG levels did not correlate with the longevity of silencing in wild-type animals and furthermore, pUGs were still present long after epigenetic silencing was undetectable (Fig. 3). The fact that silencing can be lost while pUGs are still present leads us to conclude that the presence

and maintenance of pUGs alone is not solely responsible for TEI in maintenance generations. The nuclear pathway, particularly the heterochromatic state mediated by MORC-1, is critical to maintain silencing and may act in parallel to the pUG-related pathway. Perhaps silencing is first lost at the nuclear level, while pUGs are still being produced. Germ granules are required for maintenance of functional TEI and their spatial separation is necessary for restricting the duration of TEI as animals with forcibly mixed germ granule compartments display a significant extension of TEI silencing (Zhao *et al.* 2024). Could this observation be linked with the presence of pUGs long after the end of silencing? Perhaps pUGs can be present, but sequestered and inactive in germ granule compartments and when the granules are forcibly merged, pUGs sequestration may be lifted, enabling an interaction with other factors to extend silencing longevity. Furthermore, pUGs themselves may promote the maintenance of granule stability or assembly, as we found that RDE-3 is crucial to proper granule organization (Fig. 6).

## Germ granules as organizers of TEI pathways

GLH-1 is required for the recruitment of PGL-1 to P granules and interacts with WAGO-1 in an RDE-3 dependent manner to produce WAGO-22G RNAs (Dai *et al.* 2022). P granules are the foundation granule often positioned on nuclear pores (Uebel *et al.* 2023) and are required for the formation of other granules. GLH-1 is therefore likely required for the formation of Z granules, mutator foci and SIMR foci and has been reported to direct the localization of many small RNA pathway components, including WAGO-4 and ZNFX-1 (Chen *et al.* 2022). GLH-1 also directly binds Dicer (Beshore *et al.* 2011), indicating that GLH-1 is intimately involved in RNAi-induced TEI though GLH-1's precise role in these processes is unclear.

WAGO-4 resides within both P and Z granules (Wan *et al.* 2018) and binds small RNAs. ZNFX-1 is involved in the biogenesis of pUG RNAs (Fig. 5; Ouyang *et al.* 2022) and has been suggested to sequester pools of silenced transcripts within Z granules for use as templates for sRNA amplification (Ouyang *et al.* 2022). ZNFX-1 coimmunoprecipitates with both WAGO-1 and WAGO-4. PUP-1 uridylates small RNA molecules, many of which are subsequently bound by WAGO-4 (Xu *et al.* 2018; Kelley *et al.* 2024). WAGO-4 mutants display a strong TEI defect, while both PUP-1 and ZNFX-1 mutants display less severe TEI defects than WAGO-4 (Figs. 1 and 4). This may indicate that PUP-1 and ZNFX-1 comprise separate pathways of small RNA production that converge upon WAGO-4 loading.

These key TEI proteins all reside and function within germ granules, and loss of TEI factors required in both P0 and F1 for establishment and maintenance of TEI—ZNFX-1, WAGO-4, and GLH-1—results in germ granule defects (Wan *et al.* 2018; Dai *et al.* 2022). Together, this suggests that germ granules are key organizers for the cytoplasmic element of TEI during establishment and maintenance. Correspondingly, the perturbations we observed in germ granules in RDE-3 mutants may have a significant direct effect on TEI. Alternatively, the defects may be a consequence of de-silencing of endogenous targets of RDE-3 and therefore unrelated to RNAi-induced TEI. Future work will tease apart these possibilities.

## A unified framework for RNAi-induced TEI

Ouyang *et al.* propose that 2 parallel pathways are required for TEI from the F1 generation onwards: nuclear silencing dependent on HRDE-1 and cytoplasmic silencing dependent on ZNFX-1 (Ouyang *et al.* 2022). Our data suggest the presence of another pathway involving heterochromatin formation that sits upstream of both these pathways is established in the P0 generation, and is maintained in subsequent generations. This pathway has its beginnings in heterochromatic marks such as H3K9me3 and H3K23me3 established by SET-25 and SET-32, respectively, although data suggests that the long-term maintenance of H3K9me3 is not required (Towbin *et al.* 2012; Kalinava *et al.* 2017, 2018; Woodhouse *et al.* 2018; Schwartz-Orbach *et al.* 2020). Instead, we propose that a chromatin-based silencing state maintained by MORC-1 is important in the F1 onwards. Thus, in the F1 generation onwards, there are 3 pathways required for TEI—a heterochromatin or nuclear localization-based pathway maintained by MORC-1, a cotranscriptional silencing pathway that requires HRDE-1, and a germ granule-based pathway for which ZNFX-1 is important.

## Longevity of epigenetic inheritance is determined in the P0 generation

The longevity of epigenetic inheritance differs amongst lineages from different P0 parents, while sublineages from a single P0 parent display similar but not identical inheritance dynamics (Fig. 3). This suggests that a factor in RNAi-exposed P0 parents partially determines silencing duration in their offspring, and this varies between P0 parents, consistent with the findings of Houri-Zeevi *et al.* (2020). Extending the findings of Houri-Zeevi *et al.*, we followed lineages until silencing was exhausted and selected for silenced individuals at each generation, providing novel insights into the dynamics of silencing decay and the duration of silencing. We observed a clear correlation between the proportion of silencing in the F1 generation and the longevity of epigenetic inheritance, despite variation between sublineages. This suggests that not only is silencing transmitted between generations, but also a factor which determines silencing duration. We also observed a precipitous decline in silencing around the F6 generation. This innate variation suggests that a transient factor is involved in epigenetic inheritance that can be propagated between generations and/or amplified in each generation, but that it cannot persist forever. This deciding factor may be related to the organization of germ granules, with less distinct granules allowing more interaction between silencing factors or perhaps to the expression levels of these silencing factors themselves as suggested by the correlation of HSF-1 levels with mCherry silencing in another TEI system (Houri-Zeevi *et al.* 2020). Alternatively, the strength of silencing may correlate with how well the heterochromatic state is established in the P0/F1 generation. Clearly, silencing can be lost while small RNAs targeting the gene are still present (Fig. 3; Woodhouse *et al.* 2018), and so perhaps a change in chromatin state allows production of sufficient mRNA to overwhelm small RNA silencing. Further work will be required to differentiate between these hypotheses.

## Chromatin factors with distinct roles in TEI and RNAe

Interestingly, despite the clear role for SET-25 and SET-32 in establishment of TEI, the chromatin-associated proteins MES-3, HPL-2, LET-418, and LIN-61 implicated in RNAe (Ashe *et al.* 2012; Lee *et al.* 2012; McMurchy *et al.* 2017) do not appear to be required for establishment or maintenance of TEI. HPL-2 associates with heterochromatin and regions of H3K9me1/me2, while LIN-61 binds H3K9me2 and has been shown to recruit SET-25 to some of its targets in early embryos (Padeken *et al.* 2021; de la Cruz-Ruiz *et al.* 2023). Although it is tempting to speculate that H3K9me2 and H3K9me3 play similar roles given their association with

heterochromatin, distinct functions have been observed for the 2 methylation marks during early embryogenesis (Mutlu *et al.* 2019), and loss of the histone dimethyltransferase MET-2 does not cause a loss of TEI (Woodhouse *et al.* 2018) and can even cause an increase in TEI in some systems (Lev *et al.* 2017). Our failure to observe a defect in TEI for LIN-61 and HPL-2 further highlights the different functions of H3K9me2 and H3K9me3 and the differences between RNAi-induced TEI and RNAe. Furthermore, our data suggest an additional targeting pathway for SET-25 in the germline that does not involve LIN-61. MES-3 is a component of the polycomb complex, important for mediating H3K27me3 (Shirayama *et al.* 2012) and LET-418 is a component of the NuRD complex and important for chromatin remodeling (McMurchy *et al.* 2017). Our data suggest that polycomb/H3K27me3 and the NuRD complex are not involved in RNAi-induced TEI.

Overall, these findings highlight the complexity of the molecular interactions underpinning TEI and the variability of this system will be an important focus for future research.

## Data availability

The authors affirm that all data necessary for confirming the conclusions of the article are present within the article, figures, and tables. Strains are available upon request.

Supplemental material available at GENETICS online.

## Acknowledgments

We thank the Australian Microscopy and Microanalysis Research Facility at the Australian Centre for Microscopy and Microanalysis (University of Sydney) for access to microscopes and assistance with imaging and analysis. We acknowledge Protein Production in Sydney Analytical (University of Sydney). We also thank the CGC (University of Minnesota) for strains, which is funded by NIH Office of Research Infrastructure Programs (P40 OD010440), and Wormbase (Sternberg et al. 2024).

## Funding

RMW, NF, DSM, and JJH were supported by a Research Training Program Scholarship from the Australian Government. NF was additionally supported by a Postgraduate Research Supplementary Scholarship from the Commonwealth Scientific and Industrial Research Organisation (CSIRO). AA was supported by FT180100653, DP200102904, and DP240100725 from the Australian Research Council.

## Conflicts of interest

The authors declare no conflict of interest.

## Literature cited

Akay A, Di Domenico T, Suen KM, Nabih A, Parada GE, Larance M, Medhi R, Berkyurek AC, Zhang X, Wedeles CJ, *et al.* 2017. The helicase Aquarius/EMB-4 is required to overcome intronic barriers to allow nuclear RNAi pathways to heritably silence transcription. Dev Cell. 42(3):241–255.e6. doi:10.1016/j.devcel.2017.07.002.

Arribere JA, Bell RT, Fu BXH, Artiles KL, Hartman PS, Fire AZ. 2014. Efficient marker-free recovery of custom genetic modifications with CRISPR/Cas9 in *Caenorhabditis elegans*. Genetics. 198(3): 837–846. doi:10.1534/genetics.114.169730.

Ashe A, Sapetschnig A, Weick EM, Mitchell J, Bagijn MP, Cording AC, Doebley A-L, Goldstein LD, Lehrbach NJ, Le Pen J, *et al.* 2012. piRNAs can trigger a multigenerational epigenetic memory in the germline of *C. elegans*. Cell. 150(1):88–99. doi:10.1016/j.cell.2012.06.018.

Ashe A, Sarkies P, Le Pen J, Tanguy M, Miska EA. 2015. Antiviral RNA interference against orsay virus is neither systemic nor transgenerational in *Caenorhabditis elegans*. J Virol. 89(23):12035–12046. doi:10.1128/jvi.03664-14.

Bagijn MP, Goldstein LD, Sapetschnig A, Weick EM, Bouasker S, Lehrbach NJ, Simard MJ, Miska EA. 2012. Function, targets, and evolution of *Caenorhabditis elegans* piRNAs. Science (New York, NY). 337(6094):574–578. doi:10.1126/science.1220952.

Beshore EL, McEwen TJ, Jud MC, Marshall JK, Schisa JA, Bennett KL. 2011. *C. elegans* Dicer interacts with the P-granule component GLH-1 and both regulate germline RNPs. Dev Biol. 350(2): 370–381. doi:10.1016/j.ydbio.2010.12.005.

Brenner S. 1974. The genetics of *Caenorhabditis elegans*. Genetics. 77(1):71–94. doi:10.1093/genetics/77.1.71.

Buckley Ba, Burkhart KB, Gu SG, Spracklin G, Kershner A, Fritz H, Kimble J, Fire A, Kennedy S. 2012. A nuclear argonaute promotes multigenerational epigenetic inheritance and germline immortality. Nature. 489(7416):447–451. doi:10.1038/nature11352.

Burton NO, Burkhart KB, Kennedy S. 2011. Nuclear RNAi maintains heritable gene silencing in *Caenorhabditis elegans*. Proc Natl Acad Sci USA. 108(49):19683–19688. doi:10.1073/pnas.1113310108.

Camacho J, Truong L, Kurt Z, Chen Y-W, Morselli M, Gutierrez G, Pellegrini M, Yang X, Allard P. 2018. The memory of environmental chemical exposure in *C. elegans* is dependent on the jumonji demethylases jmjd-2 and jmjd-3/utx-1. Cell Rep. 23(8): 2392–2404. doi:10.1016/J.CELREP.2018.04.078.

Chen W, Brown JS, He T, Wu W-S, Tu S, Weng Z, Zhang D, Lee H-C. 2022. GLH/VASA helicases promote germ granule formation to ensure the fidelity of piRNA-mediated transcriptome surveillance. Nat Commun. 13(1):5306. doi:10.1038/s41467-022-32880-2.

Chen X, Wang K, Mufti FUD, Xu D, Zhu C, Xinya H, Zeng C, Jin Q, Xiaona H, Yan Y, *et al.* 2024. Germ granule compartments coordinate specialized small RNA production. Nat Commun. 15(1): 5799. doi:10.1038/s41467-024-50027-3.

Dai S, Tang X, Li L, Ishidate T, Ozturk AR, Chen H, Dude AL, Yan YH, Dong MQ, Shen EZ, *et al.* 2022. A family of *C. elegans* VASA homologs control argonaute pathway specificity and promote transgenerational silencing. Cell Rep. 40(10):111265. doi:10.1016/j.celrep.2022.111265.

de la Cruz-Ruiz P, Rodríguez-Palero MJ, Askjaer P, Artal-Sanz M. 2023. Tissue-specific chromatin-binding patterns of *Caenorhabditis elegans* heterochromatin proteins HPL-1 and HPL-2 reveal differential roles in the regulation of gene expression. Genetics. 224(3): iyad081. doi:10.1093/genetics/iyad081.

Ding Y-H, Ochoa HJ, Ishidate T, Shirayama M, Mello CC. 2023. The nuclear argonaute HRDE-1 directs target gene re-localization and shuttles to nuage to promote small RNA-mediated inherited silencing. Cell Rep. 42(5):112408. doi:10.1016/j.celrep.2023.112408.

Dodson AE, Kennedy S. 2020. Phase separation in germ cells and development. Dev Cell. 55(1):4–17. doi:10.1016/j.devcel.2020.09.004.

Farboud B, Meyer BJ. 2015. Dramatic enhancement of genome editing by CRISPR/cas9 through improved guide RNA design. Genetics. 199(4):959–971. doi:10.1534/genetics.115.175166.

Farboud B, Severson AF, Meyer BJ. 2019. Strategies for efficient genome editing using CRISPR-cas9. Genetics. 211(2):431–457. doi:10.1534/genetics.118.301775.

Feng S, Jacobsen SE, Reik W. 2010. Epigenetic reprogramming in plant and animal development. Science (New York, NY). 330(6004):622. doi:10.1126/SCIENCE.1190614.

Fu BXH, Hansen LL, Artiles KL, Nonet ML, Fire AZ. 2014. Landscape of target:guide homology effects on Cas9-mediated cleavage. Nucleic Acids Res. 42(22):13778–13787. doi:10.1093/NAR/GKU1102.

Greer EL, Becker B, Latza C, Antebi A, Shi Y. 2016. Mutation of *C. elegans* demethylase spr-5 extends transgenerational longevity. Cell Res. 26(2):229–238. doi:10.1038/cr.2015.148.

Greer EL, Beese-Sims SE, Brookes E, Spadafora R, Zhu Y, Rothbart SB, Aristizábal-Corrales D, Chen S, Badeaux AI, Jin Q, *et al.* 2014. A histone methylation network regulates transgenerational epigenetic memory in *C. elegans*. Cell Rep. 7(1):113–126. doi:10.1016/j.celrep.2014.02.044.

Greer EL, Maures TJ, Ucar D, Hauswirth AG, Mancini E, Lim JP, Benayoun BA, Shi Y, Brunet A. 2011. Transgenerational epigenetic inheritance of longevity in *Caenorhabditis elegans*. Nature. 479(7373):365–371. doi:10.1038/nature10572.

Gu W, Shirayama M, Conte D, Vasale J, Batista PJ, Claycomb JM, Moresco JJ, Youngman EM, Keys J, Stoltz MJ, *et al.* 2009. Distinct argonaute-mediated 22G-RNA pathways direct genome surveillance in the *C. elegans* germline. Mol Cell. 36(2):231–244. doi:10.1016/j.molcel.2009.09.020.

Houri-Zeevi L, Kohanim YK, Antonova O, Rechavi O. 2020. Three rules explain transgenerational small RNA inheritance in *C. elegans*. Cell. 182(5):1186–1197.e12. doi:10.1016/j.cell.2020.07.022.

Ishidate T, Ozturk AR, Durning DJ, Sharma R, Shen E, Chen H, Seth M, Shirayama M, Mello CC. 2018. ZNFX-1 Functions within perinuclear nuage to balance epigenetic signals. Mol Cell. 70(4):639–649.e6. doi:10.1016/J.MOLCEL.2018.04.009.

Kaletsky R, Moore RS, Vrla GD, Parsons LR, Gitai Z, Murphy CT. 2020. *C. elegans* interprets bacterial non-coding RNAs to learn pathogenic avoidance. Nature. 586(7829):445–451. doi:10.1038/s41586-020-2699-5.

Kalinava N, Ni JZ, Gajic Z, Kim M, Ushakov H, Gu SG. 2018. *C. elegans* heterochromatin factor SET-32 plays an essential role in transgenerational establishment of nuclear RNAi-mediated epigenetic silencing. Cell Rep. 25(8):2273–2284.e3. doi:10.1016/J.CELREP.2018.10.086.

Kalinava N, Ni JZ, Peterman K, Chen E, Gu SG. 2017. Decoupling the downstream effects of germline nuclear RNAi reveals that H3K9me3 is dispensable for heritable RNAi and the maintenance of endogenous siRNA-mediated transcriptional silencing in *Caenorhabditis elegans*. Epigenetics Chromatin. 10(1):6. doi:10.1186/s13072-017-0114-8.

Kamath RS, Martinez-Campos M, Zipperlen P, Fraser AG, Ahringer J. 2000. Effectiveness of specific RNA-mediated interference through ingested double-stranded RNA in *Caenorhabditis elegans*. Genome Biol. 2(1):RESEARCH0002. doi:10.1186/gb-2000-2-1-research0002.

Kelley LH, Caldas IV, Sullenberger MT, Yongblah KE, Niazi AM, Iyer A, Li Y, Tran PM, Valen E, Ahmed-Braimah YH, *et al.* 2024. Poly(U) polymerase activity in *Caenorhabditis elegans* regulates abundance and tailing of sRNA and mRNA. Genetics. 228(2):iyae120. doi:10.1093/genetics/iyae120.

Kerr SC, Ruppersburg CC, Francis JW, Katz DJ. 2014. SPR-5 and MET-2 function cooperatively to reestablish an epigenetic ground state during passage through the germ line. Proc Natl Acad Sci USA. 111(26):9509–9514. doi:10.1073/pnas.1321843111.

Kim HJ, Yen L, Wongpalee SP, Kirshner JA, Mehta N, Xue Y, Johnston JB, Burlingame AL, Kim JK, Loparo JJ, *et al.* 2019. The gene-silencing protein MORC-1 topologically entraps DNA and forms multimeric assemblies to cause DNA compaction. Mol Cell. 75(4):700–710.e6. doi:10.1016/j.molcel.2019.07.032.

Klosin A, Reis K, Hidalgo-Carcedo C, Casas E, Vavouri T, Lehner B. 2017. Impaired DNA replication derepresses chromatin and generates a transgenerationally inherited epigenetic memory. Sci Adv. 3(8):e1701143. doi:10.1126/sciadv.1701143.

Köhler S, Dernburg A. 2016. *C. elegans* injection: Ribonucleoprotein delivery using the Alt-R CRISPR-Cas9 System. Integrated DNA Technologies.

Kumsta C, Hansen M. 2012. *C. elegans* rrf-1 mutations maintain RNAi efficiency in the soma in addition to the germline. PLoS One. 7(5):e35428. doi:10.1371/journal.pone.0035428.

Lee TW, David HS, Engstrom AK, Carpenter BS, Katz DJ. 2019. Repressive H3K9me2 protects lifespan against the transgenerational burden of COMPASS activity in *C. elegans*. eLife. 8:e48498. doi:10.7554/eLife.48498.

Lee H-C, Gu W, Shirayama M, Youngman E, Conte D, Mello CC, Mello CC. 2012. *C. elegans* piRNAs mediate the genome-wide surveillance of germline transcripts. Cell. 150(1):78–87. doi:10.1016/j.cell.2012.06.016.

Lev I, Seroussi U, Gingold H, Bril R, Anava S, Rechavi O. 2017. MET-2-dependent H3K9 methylation suppresses transgenerational small RNA inheritance. Curr Biol. 27(8):1138–1147. doi:10.1016/j.cub.2017.03.008.

Lev I, Toker IA, Mor Y, Nitzan A, Weintraub G, Antonova O, Bhonkar O, Shushan IB, Seroussi U, Claycomb JM, *et al.* 2019. Germ granules govern small RNA inheritance. Curr Biol. 29(17):2880–-2891.e4. doi:10.1016/j.cub.2019.07.054.

Lewis A, Berkyurek AC, Greiner A, Sawh AN, Vashisht A, Merrett S, Flamand MN, Wohlschlegel J, Sarov M, Miska EA, *et al.* 2020. A family of argonaute-interacting proteins gates nuclear RNAi. Mol Cell. 78(5):862–875.e8. doi:10.1016/j.molcel.2020.04.007.

Luteijn MJ, van Bergeijk P, Kaaij LJT, Almeida MV, Roovers EF, Berezikov E, Ketting RF. 2012. Extremely stable piwi-induced gene silencing in *Caenorhabditis elegans*. EMBO J. 31(16):3422–3430. doi:10.1038/emboj.2012.213.

McMurchy AN, Stempor P, Gaarenstroom T, Wysolmerski B, Dong Y, Aussianikava D, Appert A, Huang N, Kolasinska-Zwierz P, Sapetschnig A, *et al.* 2017. A team of heterochromatin factors collaborates with small RNA pathways to combat repetitive elements and germline stress. eLife. 6:e21666. doi:10.7554/eLife.21666.

Minkina O, Hunter CP. 2017. Stable heritable germline silencing directs somatic silencing at an endogenous locus. Mol Cell. 65(4):659–670.e5. doi:10.1016/j.molcel.2017.01.034.

Moore RS, Kaletsky R, Murphy CT. 2019. Piwi/PRG-1 argonaute and TGF-β mediate transgenerational learned pathogenic avoidance. Cell. 177(7):1827–1841.e12. doi:10.1016/j.cell.2019.05.024.

Mutlu B, Chen H-M, Gutnik S, Hall DH, Keppler-Ross S, Mango SE. 2019. Distinct functions and temporal regulation of methylated histone H3 during early embryogenesis. Development. 146(19):dev174516. doi:10.1242/dev.174516.

Newman MA, Ji F, Fischer SEJ, Anselmo A, Sadreyev RI, Ruvkun G. 2018. The surveillance of pre-mRNA splicing is an early step in *C. elegans* RNAi of endogenous genes. Genes Dev. 32(9–10):670–681. doi:10.1101/gad.311514.118.

Ouyang JPT, Zhang WL, Seydoux G. 2022. The conserved helicase ZNFX-1 memorializes silenced RNAs in perinuclear condensates. Nat Cell Biol. 24(7):1129–1140. doi:10.1038/s41556-022-00940-w.

Padeken J, Methot S, Zeller P, Delaney CE, Kalck V, Gasser SM. 2021. Argonaute NRDE-3 and MBT domain protein LIN-61 redundantly recruit an H3K9me3 HMT to prevent embryonic lethality and transposon expression. Genes Dev. 35(1–2):82–101. doi:10.1101/gad.344234.120.

Paix A, Wang Y, Smith HE, Lee C-YS, Calidas D, Lu T, Smith J, Schmidt H, Krause MW, Seydoux G. 2014. Scalable and Versatile genome editing using linear DNAs with micro-homology to cas9 sites in

*Caenorhabditis elegans*. Genetics. 198(4):1347–1356. doi:10.1534/genetics.114.170423.

Pereira AG, Gracida X, Kagias K, Zhang Y. 2020. *C. elegans* aversive olfactory learning generates diverse intergenerational effects. J Neurogenet. 34(3–4):378–388. doi:10.1080/01677063.2020.1819265.

Phillips CM, Montgomery TA, Breen PC, Ruvkun G. 2012. MUT-16 promotes formation of perinuclear mutator foci required for RNA silencing in the *C. elegans* germline. Genes Dev. 26(13):1433–1444. doi:10.1101/gad.193904.112.

Phillips CM, Updike DL. 2022. Germ granules and gene regulation in the *Caenorhabditis elegans* germline. Genetics. 220(3):iyab195. doi:10.1093/GENETICS/IYAB195.

Rechavi O, Houri-Ze'evi L, Anava S, Goh WSS, Kerk SY, Hannon GJ, Hobert O. 2014. Starvation-induced transgenerational inheritance of small RNAs in *C. elegans*. Cell. 158(2):277–287. doi:10.1016/j.cell.2014.06.020.

Schott D, Yanai I, Hunter CP. 2014. Natural RNA interference directs a heritable response to the environment. Sci Rep. 4(1):7387. doi:10.1038/srep07387.

Schreier J, Kielisch F, Ketting RF. 2024. A genetic framework for RNAi inheritance in *Caenorhabditis elegans*. bioRxiv 616260. https://doi.org/10.1101/2024.10.02.616260, preprint: not peer reviewed.

Schwartz-Orbach L, Zhang C, Sidoli S, Amin R, Kaur D, Zhebrun A, Ni J, Gu SG. 2020. *Caenorhabditis elegans* nuclear RNAi factor SET-32 deposits the transgenerational histone modification, H3K23me3. eLife. 9:e54309. doi:10.7554/eLife.54309.

Seroussi U, Li C, Sundby AE, Lee TL, Claycomb JM, Saltzman AL. 2022. Mechanisms of epigenetic regulation by *C. elegans* nuclear RNA interference pathways. Semin Cell Dev Biol. 127:142–154. doi:10.1016/j.semcdb.2021.11.018.

Shirayama M, Seth M, Lee H-C, Gu W, Ishidate T, Conte D, Mello CC. 2012. piRNAs initiate an epigenetic memory of nonself RNA in the *C. elegans* germline. Cell. 150(1):65–77. doi:10.1016/j.cell.2012.06.015.

Shiu PK, Hunter CP. 2017. Early developmental exposure to dsRNA is critical for initiating efficient nuclear RNAi in *C. elegans*. Cell Rep. 18(12):2969–2978. doi:10.1016/j.celrep.2017.03.002.

Shukla A, Perales R, Kennedy S. 2021. piRNAs coordinate poly(UG) tailing to prevent aberrant and perpetual gene silencing. Curr Biol. 31(20):4473–4485.e3. doi:10.1016/J.CUB.2021.07.076.

Shukla A, Yan J, Pagano DJ, Dodson AE, Fei Y, Gorham J, Seidman JGJ, Wickens M, Kennedy S. 2020. Poly(UG)-tailed RNAs in genome protection and epigenetic inheritance. Nature. 582(7811):283–288. doi:10.1038/s41586-020-2323-8.

Skvortsova K, Iovino N, Bogdanović O. 2018. Functions and mechanisms of epigenetic inheritance in animals. Nat Rev Mol Cell Biol. 19(12):774–790. doi:10.1038/s41580-018-0074-2.

Spracklin G, Fields B, Wan G, Becker D, Wallig A, Shukla A, Kennedy S. 2017. The RNAi inheritance machinery of *Caenorhabditis elegans*. Genetics. 206(3):1403–1416. doi:10.1534/genetics.116.198812.

Sternberg PW, Van Auken K, Wang Q, Wright A, Yook K, Zarowiecki M, Arnaboldi V, Becerra A, Brown S, Cain S, *et al.* 2024. WormBase 2024: status and transitioning to Alliance infrastructure. Genetics. 227(1):iyae050. doi:10.1093/genetics/iyae050.

Sundby AE, Molnar RI, Claycomb JM. 2021. Connecting the dots: linking *Caenorhabditis elegans* small RNA pathways and germ granules. Trends Cell Biol. 31(5):387–401. doi:10.1016/j.tcb.2020.12.012.

Tabara H, Sarkissian M, Kelly WG, Fleenor J, Grishok A, Timmons L, Fire A, Mello CC. 1999. The *rde-1* gene, RNA interference, and transposon silencing in *C. elegans*. Cell. 99(2):123–132. doi:10.1016/S0092-8674(00)81644-X.

Towbin BD, González-Aguilera C, Sack R, Gaidatzis D, Kalck V, Meister P, Askjaer P, Gasser SM. 2012. Step-wise methylation of histone H3K9 positions heterochromatin at the nuclear periphery. Cell. 150(5):934–947. doi:10.1016/j.cell.2012.06.051.

Tsai H-Y, Chen C-CG, Conte D, Moresco JJ, Chaves DA, Mitani S, Yates JR, Tsai M-D, Mello CC. 2015. A ribonuclease coordinates siRNA amplification and mRNA cleavage during RNAi. Cell. 160(3):407–419. doi:10.1016/j.cell.2015.01.010.

Tyc KM, Nabih A, Wu MZ, Wedeles CJ, Sobotka JA, Claycomb JM. 2017. The conserved intron binding protein EMB-4 plays differential roles in germline small RNA pathways of *C. elegans*. Dev Cell. 42(3):256–270.e6. doi:10.1016/j.devcel.2017.07.003.

Uebel CJ, Rajeev S, Phillips CM. 2023. *Caenorhabditis elegans* germ granules are present in distinct configurations and assemble in a hierarchical manner. Development. 150(24):dev202284. doi:10.1242/dev.202284.

Vastenhouw NL, Brunschwig K, Okihara KL, Müller F, Tijsterman M, Plasterk RHA. 2006. Gene expression: long-term gene silencing by RNAi. Nature. 442(7105):882. doi:10.1038/442882a.

Wan G, Fields BD, Spracklin G, Shukla A, Phillips CM, Kennedy S. 2018. Spatiotemporal regulation of liquid-like condensates in epigenetic inheritance. Nature. 557(7707):679–683. doi:10.1038/s41586-018-0132-0.

Wan QL, Meng X, Dai W, Luo Z, Wang C, Fu X, Yang J, Ye Q, Zhou Q. 2021. N6-methyldeoxyadenine and histone methylation mediate transgenerational survival advantages induced by hormetic heat stress. Sci Adv. 7(1):eabc3026. doi:10.1126/sciadv.abc3026.

Wan G, Yan J, Fei Y, Pagano DJ, Kennedy S. 2020. A conserved NRDE-2/MTR-4 Complex mediates nuclear RNAi in *Caenorhabditis elegans*. Genetics. 216(4):1071–1085. doi:10.1534/genetics.120.303631.

Weiser NE, Yang DX, Feng S, Kalinava N, Brown KC, Khanikar J, Freeberg MA, Snyder MJ, Csankovszki G, Chan RC, *et al.* 2017. MORC-1 Integrates nuclear RNAi and transgenerational chromatin architecture to promote germline immortality. Dev Cell. 41(4):408–423.e7. doi:10.1016/J.DEVCEL.2017.04.023.

Woodhouse RM, Ashe A. 2019. Transgenerational epigenetic inheritance is revealed as a multi-step process by studies of the SET-domain proteins SET-25 and SET-32. Epigenet Insights. 12:2516865719844214. doi:10.1177/2516865719844214.

Woodhouse RM, Buchmann GG, Hoe M, Harney DJ, Low JKK, Larance M, Boag PR, Ashe A, Low JKK, Larance M, *et al.* 2018. Chromatin modifiers SET-25 and SET-32 are required for establishment but not long-term maintenance of transgenerational epigenetic inheritance. Cell Rep. 25(8):2259–2272.e5. doi:10.1101/255646.

Xu F, Feng X, Chen X, Weng C, Yan Q, Xu T, Hong M, Guang S. 2018. A cytoplasmic argonaute protein promotes the inheritance of RNAi. Cell Rep. 23(8):2482–2494. doi:10.1016/J.CELREP.2018.04.072.

Zhao C, Cai S, Shi R, Li X, Deng B, Li R, Yang S, Huang J, Liang Y, Lu P, *et al.* 2024. HERD-1 mediates multiphase condensate immiscibility to regulate small RNA-driven transgenerational epigenetic inheritance. Nat Cell Biol. 26(11):1958–1970. doi:10.1038/s41556-024-01514-8.

*Editor: G. Seydoux*